

Fisher Information Maximization for Distributed Vector Estimation in Wireless Sensor Networks

Mojtaba Shirazi, Azadeh Vosoughi, *Senior Member, IEEE*

Abstract—In this paper we consider the problem of distributed estimation of a Gaussian vector with linear observation model in a wireless sensor network (WSN). Each sensor employs a uniform multi-bit quantizer to quantize its noisy observation, maps it to a digitally modulated symbol, and transmits the symbol over power-constrained wireless channels (subject to fading and noise) to a fusion center (FC), which is tasked with fusing the received signals and estimating the unknown vector. We derive the Bayesian Fisher Information Matrix (FIM) from the collectively received signals at the FC, and also, the mean square error (MSE) of the linear minimum mean square error (LMMSE) estimator. Our derivations reveal how these two metrics depend on the observation model and its parameters, and the physical layer parameters (e.g., modulation scheme, receiver type at the FC, channel gain, channel noise, transmit power, and quantization bits). Moreover, we study two transmit power allocation schemes that maximize trace and log-determinant of FIM under network transmit power constraint (which we refer to as FIM-max schemes). In our simulations, we evaluate the system performance in terms of MSE using the solutions of FIM-max schemes, and compare it with the solution obtained from minimizing the MSE of the LMMSE estimator (MSE-min scheme), and that of uniform power allocation. We investigate how the power allocation depends on the sensors observation qualities and physical layer parameters as well as the network transmit power constraint. Our simulations demonstrate the efficiency of FIM-max schemes, as MSE distortions associated with FIM-max schemes are very close to that of MSE-min scheme and outperform that of uniform power allocation in all simulation scenarios. We also compare the performances of coherent and noncoherent receivers with known channel envelopes as well as known channel statistics. Numerical results reveal that coherent receiver and noncoherent receiver with known channel statistics have the best and the worst performance, respectively.

Index Terms—Distributed estimation, Gaussian vector, Bayesian Fisher Information Matrix, LMMSE estimator, coherent versus noncoherent receiver, power allocation, linear observation model.

I. INTRODUCTION

The large plethora of wireless sensor network (WSN) applications, with practical constraints on network power and bandwidth raises a series of challenging technical problems for system engineers. One of these problems is distributed parameter estimation, where geographically distributed battery-powered sensors are deployed over a sensing field to monitor physical or environmental conditions [1]. One of the research thrusts in the field of distributed parameter estimation is designing optimal quantization strategies, assuming that sensors' observations are sent over bandwidth constrained (otherwise error-free) communication channels. For example [2], [3] found the minimum achievable Cramér-Rao bound

(CRB) and the optimal quantizers for estimating a *deterministic scalar*, assuming identical one-bit quantizers. [4], [5] studied the problem for a *deterministic scalar* based on one-bit or multi-bit quantizers. The aforementioned works, however, assume that the bandwidth constrained communication channels carrying sensors' data are *error-free* and in most cases consider only homogeneous sensors. The authors in [6], [7] studied this problem for *erroneous* bandwidth constrained channels. In particular, this problem was investigated in [6] for a *deterministic scalar* and in [7] for an unknown *Gaussian scalar*, based on quantization of correlated observations. Note that modeling the unknown parameter to be estimated as random (instead of deterministic) allows the system designer to incorporate *a priori* statistical knowledge and to exploit the correlation among sensors' observation. When addressing the problem, these works assume a linear estimator at the fusion center (FC) and studied the mean square error (MSE) distortion pertaining to this linear estimator: the authors in [4]–[6] considered the best linear unbiased estimator (BLUE) and the authors in [7] considered the linear minimum mean square error (LMMSE) estimator. Departing from the idealistic assumption of error-free communication channels, [8] studied an iterative expectation-maximization algorithm and the CRB when sensors employ fixed and identical multi-bit quantizers and the communication channel model is additive white Gaussian noise (AWGN). A related problem was studied in [9], in which the FC employs a spatial BLUE for field reconstruction and the MSE is compared with a posterior CRB. Another research thrust in the field of distributed parameter estimation is optimizing a distributed sensor network with respect to energy consumption during transmission. In [6], the authors explored the optimal power allocation scheme that minimizes network transmission energy, subject to a target MSE constraint. On the contrary, [10], [11] minimized the MSE subject to a network transmit power constraint. For estimating a *deterministic scalar*, [10] considered a BLUE estimator and obtained the optimal quantization rate and transmission energy for active sensors. For a power constrained sensor network with homogeneous sensors, [11] investigated the optimal bit and power allocation scheme that minimizes the MSE, when communication links are modeled as binary symmetric channels (BSCs). In the most recent works [7], [12], the authors proposed joint power and rate allocation schemes for *distributed scalar* [7] and *vector* [12] estimation problems in a WSN with heterogeneous sensors, where they minimized an upper bound on the MSE of the LMMSE estimator.

Alternatively, one can consider the CRB, which is widely employed to evaluate the fundamental limits of a (distributed)

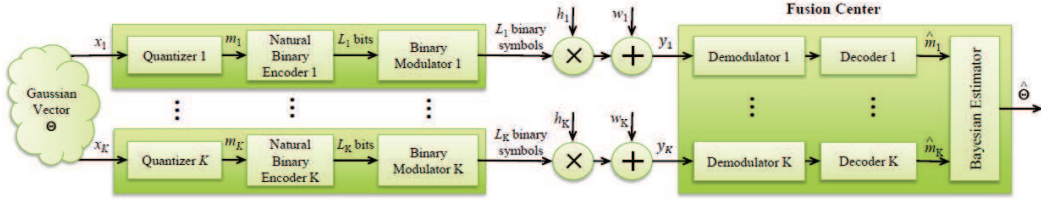


Fig. 1: Our system model consists of K sensors and a FC, that is tasked with estimating a Gaussian vector θ , via fusing collective received signals.

parameter estimation problem. For random (deterministic) unknown parameters, Bayesian (classic) CRB has been used to set a lower bound on the MSE of any Bayesian (unbiased) estimator [13]. In [14] [15], we presented our preliminary results on deriving Bayesian CRB and studied its behavior with respect to the system parameters for distributed estimation of a Gaussian vector with linear observation model, and a non-Gaussian vector with nonlinear observation model.

Considering distributed estimation of a Gaussian vector with linear observation model, we derive Bayesian Fisher Information Matrix (FIM). Our derivations unveil how the Bayesian FIM depends on the observation model and its parameters as well as the physical layer parameters. We study the optimal transmit power allocation schemes via maximizing trace and log-determinant of FIM subject to network transmit power constraint (which we refer to as FIM-max schemes). We also link the constrained maximization of log-determinant of FIM, to the constrained maximization of mutual information between the unknown vector and its Bayesian estimator. Within the context of distributed parameter estimation, maximizing FIM has been adopted before to address sensor selection [16] and optimal quantization design [17]. In particular, [16] investigated the optimal sensor activation strategy in a network with linear observation model and correlated measurement noises, via maximizing trace of FIM subject to energy constraints. [17] explored the optimal score-function based quantization that maximizes FIM corresponding to estimating a *deterministic scalar*. We derive the MSE corresponding to the LMMSE estimator at the FC for both coherent and noncoherent receivers. For both receivers, we show that the MSE corresponding to the proposed FIM-max schemes are very close to the MSE corresponding to power allocation that minimizes the MSE expression itself. Furthermore, we show that the MSE corresponding to the proposed FIM-max schemes are superior to uniform power allocation, confirming the significance of the proposed FIM-max schemes.

The remainder of this paper is organized as follows. Section II introduces our system model and formulates two constrained optimization problems, namely, maximization of trace and log-determinant of FIM, subject to network transmit power constraint. Section III links Bayesian FIM to mutual information between the unknown vector and its Bayesian estimator. Section IV derives the Bayesian FIM in terms of the optimization parameters, i.e., transmit power per sensor. Section V characterizes the MSE corresponding to the LMMSE estimator. Section VI discusses our solution methodologies to address the proposed constrained maximization problems. Section VII presents our simulation results. Section VIII concludes our work.

Notations: Throughout this paper, matrices are denoted by bold uppercase letters, vectors by bold lowercase letters, and scalars by normal letters. Note that \mathbb{E} denotes the mathematical expectation operator, $\|\cdot\|$ and $[\cdot]^T$ represent the L^2 norm of a vector and the matrix-vector transpose operation, respectively. $\text{tr}(\cdot)$ and $|\cdot|$ indicate trace and determinant of a matrix, respectively, and $|\mathcal{A}|$ is the cardinality of set \mathcal{A} .

II. SYSTEM MODEL AND PROBLEM STATEMENT

We consider a network with the system model shown in Fig. 1. Suppose there are K spatially-distributed and inhomogeneous sensors, each making a noisy observation of a common unobservable zero-mean Gaussian vector $\theta = [\theta_1, \theta_2, \dots, \theta_q]^T \in \mathbb{R}^q$ with covariance matrix $\mathbf{C}_\theta = \mathbb{E}\{\theta\theta^T\}$. Let x_k denote scalar noisy observation of sensor k . For linear observation model we have:

$$x_k = \mathbf{a}_k^T \theta + n_k, \quad k = 1, \dots, K \quad (1)$$

where $\mathbf{a}_k = [a_{k1}, a_{k2}, \dots, a_{kq}]^T \in \mathbb{R}^q$ is known observation gain vector and n_k denotes zero-mean Gaussian observation noise with variance $\sigma_{n_k}^2$. We assume that n_k 's are uncorrelated across the sensors and also are uncorrelated with θ . Sensor k employs a uniform scalar quantizer¹ with $M_k = 2^{L_k}$ quantization levels $m_{k,l} = \frac{(2l-1-M_k)\Delta_k}{2}$ for $l = 1, \dots, M_k$, where Δ_k denotes the quantization step size and index l indicates the quantization level $m_{k,l}$. We assume x_k lies in the interval $[-\tau_k, \tau_k]$ almost surely, for some reasonably large τ_k , and we have $p(|x_k| \geq \tau_k) \approx 0$. Hence, we choose $\Delta_k = \frac{2\tau_k}{(2^{L_k}-1)}$ [7], [12]. The quantizer maps x_k to one of the quantization levels $m_k \in \{m_{k,1}, \dots, m_{k,M_k}\}$ as the following:

$$m_k = m_{k,l}, \quad \text{for } x_k \in [u_{k,l}, u_{k,l+1}], \quad l = 1, \dots, M_k$$

where $u_{k,l} = \frac{(2l-2-M_k)\Delta_k}{2}$, $l = 2, \dots, M_k$, are quantization boundaries with $u_{k,1}$ and u_{k,M_k+1} denoting the largest lower bound and the smallest upper bound on x_k , respectively. We let $u_{k,1} = -\infty$ and $u_{k,M_k+1} = +\infty$. Following quantization, sensor k employs a fixed length encoder, which encodes the index l corresponding to the quantization level $m_{k,l}$ to a binary sequence of length $L_k = \log_2 M_k$ according to natural binary encoding² [7], [12], and finally modulates these L_k bits into L_k binary symbols. Let P_k denote the average transmit power corresponding to L_k symbols from sensor k , which is equally distributed among L_k symbols. We consider two types of modulators, Binary Phase Shift Keying (BPSK) modulator, which maps each bit of L_k -bit sequence into one symbol with

¹Uniform quantization is needed for Widrow's approximation in section IV and enabling the derivations of FIM.

²Natural binary encoding is needed to enable the derivations of FIM and (23) in subsection IV-C.

transmit power P_k/L_k , and On-Off Keying (OOK) modulator, which maps each “1” bit of L_k -bit sequence into one symbol with transmit power $2P_k/L_k$ and sends no carrier for “0” bit.

Sensors send their modulated symbols to the FC over orthogonal flat fading channels, with fading coefficient $h_k = |h_k|e^{j\phi_k}$. We assume that channel h_k remains constant during the transmission of L_k symbols. Denote $w_{k,i}$ as communication channel noise during the transmission of i -th symbol of L_k symbols corresponding to sensor k . We assume $w_{k,i}$'s are independent across k channels and independent and identically distributed (i.i.d.) across L_k transmitted symbols, $w_{k,i} \sim \mathcal{CN}(0, 2\sigma_{w_k}^2)$. We further assume that there is a constraint on the network transmit power, i.e., $\sum_{k=1}^K P_k \leq P_{tot}$.

To describe the estimation operation at the FC, let \hat{m}_k denote the recovered quantization level corresponding to sensor k , where in general, $\hat{m}_k \neq m_k$ due to communication channel errors. The FC processes the channel output corresponding to sensor k to recover the transmitted quantization levels $\hat{m}_k \in \{\hat{m}_{k,1}, \dots, \hat{m}_{k,M_k}\}$. We consider coherent and noncoherent receivers, corresponding to BPSK and OOK modulation schemes, respectively. For noncoherent receiver, we consider two scenarios: a) channel envelopes $|h_k|$'s are available at the FC [18], b) only statistics of complex Gaussian channel are available [19]. Having $\{\hat{m}_1, \dots, \hat{m}_K\}$, the FC applies a Bayesian estimator to form the estimate $\hat{\theta}$. Define vector $\mathbf{m} = [m_1, \dots, m_K]^T$ which consists of transmitted quantization levels, and vector $\hat{\mathbf{m}} = [\hat{m}_1, \dots, \hat{m}_K]^T$ that includes recovered quantization levels at the FC. Let $p(\hat{\mathbf{m}}, \theta)$ denote the joint probability distribution function (pdf) of the recovered quantization levels and unknown vector θ . Under certain regularity conditions that are satisfied by Gaussian vectors, the $q \times q$ FIM, denoted as \mathbf{J} , is defined as [13], [20], [21]:

$$\mathbf{J} = \mathbb{E} \left\{ \left(\frac{\partial \ln p(\hat{\mathbf{m}}, \theta)}{\partial \theta} \right) \left(\frac{\partial \ln p(\hat{\mathbf{m}}, \theta)}{\partial \theta} \right)^T \right\}, \quad (2)$$

where the expectation is taken over $p(\hat{\mathbf{m}}, \theta)$.

Our goals are to derive \mathbf{J} in closed form expression and study the transmit power allocation that maximizes either $\text{tr}(\mathbf{J})$ or $|\mathbf{J}|$ [16], [22], subject to the network transmit power constraint (FIM-max schemes). In other words, we are interested in solving the following constrained optimization problems:

$$\begin{aligned} & \underset{P_k, \forall k}{\text{maximize}} && \text{tr}(\mathbf{J}(\{P_k\}_{k=1}^K)) \\ & \text{s.t.} && \sum_{k=1}^K P_k \leq P_{tot}, \quad P_k \in \mathbb{R}^+, \quad \forall k \end{aligned} \quad (3)$$

and

$$\begin{aligned} & \underset{P_k, \forall k}{\text{maximize}} && \log |\mathbf{J}(\{P_k\}_{k=1}^K)| \\ & \text{s.t.} && \sum_{k=1}^K P_k \leq P_{tot}, \quad P_k \in \mathbb{R}^+, \quad \forall k \end{aligned} \quad (4)$$

III. LINKING FIM TO MUTUAL INFORMATION

The constrained maximization problem in (4) can be linked to the constrained maximization of mutual information between the unknown θ and its Bayesian estimate $\hat{\theta}$. Let

$\tilde{\theta} = \theta - \hat{\theta}$ where $\tilde{\theta}$ is the corresponding estimation error vector. Suppose $\boldsymbol{\mu} = \mathbb{E}\{\tilde{\theta}\}$ and $\mathcal{D} = \mathbb{E}\{\tilde{\theta}\tilde{\theta}^T\}$ are the error mean vector and the MSE matrix, respectively. We write:

$$\begin{aligned} I(\theta; \hat{\theta}) &= \mathcal{H}(\theta) - \mathcal{H}(\theta|\hat{\theta}) \\ &= \mathcal{H}(\theta) - \mathcal{H}(\theta - \hat{\theta}|\hat{\theta}) \end{aligned} \quad (5)$$

$$\geq \mathcal{H}(\theta) - \mathcal{H}(\tilde{\theta}) \quad (6)$$

$$\geq \mathcal{H}(\theta) - \log_2(|\pi e(\mathcal{D} - \boldsymbol{\mu}\boldsymbol{\mu}^T)|) \quad (7)$$

$$\geq \mathcal{H}(\theta) - q \log_2(\pi e) - \log_2(|\mathcal{D}|), \quad (8)$$

using the facts that in (5) adding a constant does not change the entropy, in (6) conditioning reduces the entropy, in (7) the entropy of a random vector with a given covariance matrix is upper bounded by the entropy of a Gaussian random vector with the same covariance matrix [23], and in (8) $\log|\cdot|$ is an increasing function on the cone of positive definite Hermitian matrices [23]. On the other hand, assuming the regularity conditions hold [20], the inverse of FIM establishes a lower bound on the MSE matrix \mathcal{D} . The Bayesian Cramér-Rao inequality states [20]:

$$\mathcal{D} \succeq \mathbf{J}^{-1}.$$

Using the concavity of the function $\log|\cdot|$ on the cone of positive definite Hermitian matrices [23], we conclude that the lower bound on $I(\theta; \hat{\theta})$ is maximized if we substitute \mathcal{D} in (8) with \mathbf{J}^{-1} . In other words:

$$I(\theta; \hat{\theta}) \geq \mathcal{H}(\theta) - q \log_2(\pi e) + \log_2(|\mathbf{J}|). \quad (9)$$

Based on (9), we observe that the problem in (4) is equivalent to maximization of the mutual information lower bound.

IV. CHARACTERIZATION OF FIM

In this section, we characterize \mathbf{J} in terms of the optimization parameters $P_k, \forall k$. The matrix \mathbf{J} in (2) can be decomposed into two terms [13], [21]:

$$\mathbf{J} = \mathbb{E}\{\boldsymbol{\Omega}(\theta)\} + \mathbb{E}\{\boldsymbol{\Lambda}(\theta)\}, \quad (10)$$

in which the expectations are taken over θ . The $q \times q$ matrix $\boldsymbol{\Omega}(\theta)$ only depends on the pdf of θ , denoted as $f(\theta)$ [13]. In particular, let $[\boldsymbol{\Omega}(\theta)]_{ij}$ denote the (i, j) -th entry of matrix $\boldsymbol{\Omega}(\theta)$. We have:

$$[\boldsymbol{\Omega}(\theta)]_{ij} = -\frac{\partial^2 \ln f(\theta)}{\partial \theta_i \partial \theta_j}, \quad i, j = 1, \dots, q$$

Since θ is zero-mean Gaussian with covariance matrix \mathbf{C}_θ , we obtain $\mathbb{E}\{\boldsymbol{\Omega}(\theta)\} = \mathbf{C}_\theta^{-1}$. Let $[\boldsymbol{\Lambda}(\theta)]_{ij}$ represent the (i, j) -th entry of matrix $\boldsymbol{\Lambda}(\theta)$. We can write:

$$[\boldsymbol{\Lambda}(\theta)]_{ij} = -\mathbb{E} \left\{ \frac{\partial^2 \ln p(\hat{\mathbf{m}}|\theta)}{\partial \theta_i \partial \theta_j} \right\}, \quad i, j = 1, \dots, q \quad (11)$$

We note that the entries $[\boldsymbol{\Lambda}(\theta)]_{ij}$ depend on the parameters of observation model as well as the physical layer parameters (e.g., modulation scheme, receiver type, channel gain, channel noise, transmit power, and quantization bits). To find $[\boldsymbol{\Lambda}(\theta)]_{ij}$ in (11), first, we show that, given θ , the entries of vector $\hat{\mathbf{m}}$ are independent, i.e., $p(\hat{\mathbf{m}}|\theta) = \prod_{k=1}^K p(\hat{m}_k|\theta)$. Since additive observation noises n_k 's are uncorrelated across the sensors and also uncorrelated with θ , we have:

$$f(\mathbf{x}|\boldsymbol{\theta}) = \prod_{k=1}^K f(x_k|\boldsymbol{\theta}). \quad (12)$$

Furthermore, we can model vector $\hat{\mathbf{m}}$ as [24]:

$$\hat{\mathbf{m}} = \mathbf{m} + \boldsymbol{\nu}, \quad (13)$$

where channel error vector $\boldsymbol{\nu} = [\nu_1, \dots, \nu_K]^T$ includes the effect of erroneous communication channels, and therefore it is reasonable to assume $\boldsymbol{\nu}$ is independent of \mathbf{m} and $\boldsymbol{\theta}$. For sensor k , let the difference between observation x_k and its quantization level m_k , i.e., $\epsilon_k = m_k - x_k$ be the corresponding quantization noise. We define $\mathbf{x} = [x_1, \dots, x_K]^T$ and $\boldsymbol{\epsilon} = [\epsilon_1, \dots, \epsilon_K]^T$, respectively as observation vector and vector of quantization noises. Then, the vector \mathbf{m} can be modeled as [12]:

$$\mathbf{m} = \mathbf{x} + \boldsymbol{\epsilon}. \quad (14)$$

Combining (13) and (14) we can write:

$$p(\hat{\mathbf{m}}|\boldsymbol{\theta}) = p(\mathbf{x} + \boldsymbol{\epsilon} + \boldsymbol{\nu}|\boldsymbol{\theta}), \quad (15)$$

In general, ϵ_k 's are mutually correlated across the sensors and also are correlated with x_k 's. However, in [25] it is shown that, when correlated Gaussian random variables are quantized with uniform quantizers of step sizes Δ_k 's, quantization noises can be approximated as mutually independent random variables, that are uniformly distributed in the interval $[-\frac{\Delta_k}{2}, \frac{\Delta_k}{2}]$, and are also independent of quantizer inputs. Here, since $\boldsymbol{\theta}$ and n_k 's in (1) are assumed Gaussian, x_k 's are correlated Gaussian that are quantized with uniform quantizers of quantization step sizes Δ_k 's. Hence, similar to [12], we approximate ϵ_k 's as mutually independent zero mean uniform random variables with variance $\sigma_{\epsilon_k}^2 = \frac{\Delta_k^2}{12}$, that are also independent of x_k 's (and thus independent of $\boldsymbol{\theta}$ and n_k 's). We refer to this approximation as *Widrow's approximation*.

Combining all above assumptions and Widrow's approximation we conclude \mathbf{x} , $\boldsymbol{\epsilon}$, $\boldsymbol{\nu}$ are mutually independent, and also, $\boldsymbol{\epsilon}$ and $\boldsymbol{\nu}$ are independent of $\boldsymbol{\theta}$. Therefore, we can write:

$$p(\hat{\mathbf{m}}|\boldsymbol{\theta}) = \prod_{k=1}^K p(\hat{m}_k|\boldsymbol{\theta}). \quad (16)$$

Substituting (16) in (11) yields:

$$[\mathbf{\Lambda}(\boldsymbol{\theta})]_{ij} = -\mathbb{E} \left\{ \sum_{k=1}^K \left[\frac{1}{p(\hat{m}_k|\boldsymbol{\theta})} \frac{\partial^2 p(\hat{m}_k|\boldsymbol{\theta})}{\partial \theta_i \partial \theta_j} - \frac{1}{p^2(\hat{m}_k|\boldsymbol{\theta})} \frac{\partial p(\hat{m}_k|\boldsymbol{\theta})}{\partial \theta_i} \frac{\partial p(\hat{m}_k|\boldsymbol{\theta})}{\partial \theta_j} \right] \right\}, \quad i, j = 1, \dots, q$$

where the expectation is taken with respect to $p(\hat{\mathbf{m}}|\boldsymbol{\theta})$, that is:

$$[\mathbf{\Lambda}(\boldsymbol{\theta})]_{ij} = -\sum_{\hat{\mathbf{m}}_1} \dots \sum_{\hat{\mathbf{m}}_K} \left\{ \sum_{k=1}^K \left[\frac{\partial^2 p(\hat{m}_k|\boldsymbol{\theta})}{\partial \theta_i \partial \theta_j} - \frac{1}{p(\hat{m}_k|\boldsymbol{\theta})} \frac{\partial p(\hat{m}_k|\boldsymbol{\theta})}{\partial \theta_i} \frac{\partial p(\hat{m}_k|\boldsymbol{\theta})}{\partial \theta_j} \right] \right\} \prod_{\substack{n=1 \\ n \neq k}}^K p(\hat{m}_n|\boldsymbol{\theta}).$$

Using the following two facts:

$$\sum_{\hat{m}_1} \dots \sum_{\hat{m}_{k-1}} \sum_{\hat{m}_{k+1}} \dots \sum_{\hat{m}_K} \prod_{\substack{n=1 \\ n \neq k}}^K p(\hat{m}_n|\boldsymbol{\theta}) = 1, \\ \sum_{k=1}^K \sum_{t=1}^{M_k} \frac{\partial^2 p(\hat{m}_{k,t}|\boldsymbol{\theta})}{\partial \theta_i \partial \theta_j} = \sum_{k=1}^K \frac{\partial^2}{\partial \theta_i \partial \theta_j} \left(\underbrace{\sum_{t=1}^{M_k} p(\hat{m}_{k,t}|\boldsymbol{\theta})}_{=1} \right) = 0,$$

where index t indicates the quantization level corresponding to \hat{m}_k , we find that $[\mathbf{\Lambda}(\boldsymbol{\theta})]_{ij}$ reduces to:

$$[\mathbf{\Lambda}(\boldsymbol{\theta})]_{ij} = \sum_{k=1}^K \sum_{t=1}^{M_k} \left(\frac{1}{p(\hat{m}_{k,t}|\boldsymbol{\theta})} \frac{\partial p(\hat{m}_{k,t}|\boldsymbol{\theta})}{\partial \theta_i} \frac{\partial p(\hat{m}_{k,t}|\boldsymbol{\theta})}{\partial \theta_j} \right). \quad (17)$$

Examining (17) we realize that we need to find two terms in order to fully characterize $[\mathbf{\Lambda}(\boldsymbol{\theta})]_{ij}$: the probability term $p(\hat{m}_{k,t}|\boldsymbol{\theta})$, and its first derivative with respect to θ_i , i.e., $\partial p(\hat{m}_{k,t}|\boldsymbol{\theta})/\partial \theta_i$. In the following, we derive these two terms.

A. Characterizing $p(\hat{m}_{k,t}|\boldsymbol{\theta})$ in (17)

To find $p(\hat{m}_{k,t}|\boldsymbol{\theta})$, first we show that $\boldsymbol{\theta}$, \mathbf{m} and $\hat{\mathbf{m}}$ form a Markov chain³. Based on what we have described so far, we can write:

$$p(\hat{\mathbf{m}}, \boldsymbol{\theta}|\mathbf{m}) = p(\mathbf{m} + \boldsymbol{\nu}, \boldsymbol{\theta}|\mathbf{m}) = p(\hat{\mathbf{m}}|\mathbf{m})p(\boldsymbol{\theta}|\mathbf{m}).$$

Hence, $\boldsymbol{\theta}$, \mathbf{m} and $\hat{\mathbf{m}}$ form a Markov chain and $p(\hat{m}_{k,t}|\mathbf{m}_{k,l}, \boldsymbol{\theta}) = p(\hat{m}_{k,t}|\mathbf{m}_{k,l})$, where index l indicates the quantization level corresponding to m_k . Using this Markov chain, we can express:

$$p(\hat{m}_{k,t}|\boldsymbol{\theta}) = \sum_{l=1}^{M_k} \underbrace{p(\hat{m}_{k,t}|\mathbf{m}_{k,l})}_{=\alpha_{k,t,l}} \underbrace{p(\mathbf{m}_{k,l}|\boldsymbol{\theta})}_{=\beta_{k,l}(\boldsymbol{\theta})}, \quad t=1, \dots, M_k \quad (18)$$

Considering $p(\hat{m}_{k,t}|\boldsymbol{\theta})$ in (18) we realize that each term inside the sum is the product of two probabilities: the first probability $\alpha_{k,t,l}$ does not depend on $\boldsymbol{\theta}$; it depends on the modulation scheme (BPSK or OOK) and the receiver type at the FC (coherent or noncoherent) as well as the physical layer parameters, i.e., channel errors due to fading and noise, transmit power P_k , and number of transmitted bits L_k . On the other hand, the second probability $\beta_{k,l}(\boldsymbol{\theta})$ depends on $\boldsymbol{\theta}$, the observation model and its parameters as well as quantizer. In other words, the contributions of the observation model and quantization in each term inside the sum in (18) are *decoupled* from those of communication system.

B. Deriving $\beta_{k,l}(\boldsymbol{\theta})$ in (18) and $\partial p(\hat{m}_{k,t}|\boldsymbol{\theta})/\partial \theta_i$ in (17)

By definition, we have:

$$\beta_{k,l}(\boldsymbol{\theta}) = \int_{u_{k,l}}^{u_{k,l+1}} f(x_k|\boldsymbol{\theta}) dx_k, \quad (19)$$

where the integration bounds are the quantization boundaries and $f(x_k|\boldsymbol{\theta})$ is the conditional pdf of random variable x_k given $\boldsymbol{\theta}$, which is $\mathcal{N}(\mathbf{a}_k^T \boldsymbol{\theta}, \sigma_{n_k}^2)$. For Gaussian additive observation noise n_k , the uniform quantizer described in Section

³We say that random variables x, y, z form a Markov chain, denoted by $x \rightarrow y \rightarrow z$, if Markov property holds $p(z|x, y) = p(z|y)$ [23].

II, and using the assumption we made earlier that n_k is independent of θ , $\beta_{k,l}(\theta)$ can be computed as below:

$$\beta_{k,l}(\theta) = Q\left(\frac{u_{k,l} - \mathbf{a}_k^T \theta}{\sigma_{n_k}}\right) - Q\left(\frac{u_{k,l+1} - \mathbf{a}_k^T \theta}{\sigma_{n_k}}\right). \quad (20)$$

Next, we find $\partial p(\hat{m}_{k,t}|\theta)/\partial \theta_i$ in (17). Since $\alpha_{k,t,l}$ does not depend on θ , from (18) we have:

$$\frac{\partial p(\hat{m}_{k,t}|\theta)}{\partial \theta_i} = \sum_{l=1}^{M_k} \alpha_{k,t,l} \frac{\partial \beta_{k,l}(\theta)}{\partial \theta_i}, \quad i = 1, \dots, q \quad (21)$$

where the first derivative of $\beta_{k,l}(\theta)$ can be found using (20):

$$\begin{aligned} \frac{\partial \beta_{k,l}(\theta)}{\partial \theta_i} &= \frac{a_{k,i}}{\sqrt{2\pi}\sigma_{n_k}} \dot{\beta}_{k,l}(\theta), \quad l = 1, \dots, M_k \\ \dot{\beta}_{k,l}(\theta) &= \exp\left(-\frac{(u_{k,l} - \mathbf{a}_k^T \theta)^2}{2\sigma_{n_k}^2}\right) - \exp\left(-\frac{(u_{k,l+1} - \mathbf{a}_k^T \theta)^2}{2\sigma_{n_k}^2}\right). \end{aligned} \quad (22)$$

C. Characterizing $\alpha_{k,t,l}$ in (18)

As we mentioned before, $\alpha_{k,t,l}$ depends on the modulation scheme and the type of receiver at the FC. In this section we derive $\alpha_{k,t,l}$ for BPSK modulation with coherent receiver and OOK modulation with noncoherent receiver. For OOK modulation with noncoherent receiver, we consider two scenarios: a) channel envelopes are available at the FC, b) channel envelopes are unavailable at the FC and only channel statistics are available. We assume that the FC performs a symbol-by-symbol demodulation. To enable derivations of $\alpha_{k,t,l}$, we write $m_{k,l}$ and $\hat{m}_{k,t}$ using their corresponding bit representations in natural binary coding:

$$m_{k,l} = \sum_{i=1}^{L_k} b_{k,l,i} 2^{L_k-i}, \quad \hat{m}_{k,t} = \sum_{i=1}^{L_k} b_{k,t,i} 2^{L_k-i}. \quad (23)$$

where $[b_{k,l,1}, \dots, b_{k,l,L_k}]$ and $[b_{k,t,1}, \dots, b_{k,t,L_k}]$, respectively, are the transmitted bit sequence and recovered (received) bit sequence of sensor k .

1) *Coherent Receiver*: Suppose the Hamming distance between two bit sequences $[b_{k,l,1}, \dots, b_{k,l,L_k}]$ and $[b_{k,t,1}, \dots, b_{k,t,L_k}]$ is $N_{e_{k,t,l}} = \sum_{i=1}^{L_k} b_{k,t,i} \oplus b_{k,l,i}$, in which \oplus is the Boolean sum operator. Let γ_k be the channel signal to noise ratio (SNR) of sensor k , where:

$$\gamma_k = \frac{P_k |h_k|^2}{2L_k \sigma_{w_k}^2}. \quad (24)$$

We can model the channel between sensor k and the FC as a BSC with a bit error probability, i.e., probability of flipping a bit, $\mathcal{E}_k = Q(\sqrt{2\gamma_k})$, where $Q(x) = \frac{1}{\sqrt{2\pi}} \int_x^\infty e^{-\frac{u^2}{2}} du$ and \mathcal{E}_k does not depend on the bit index. Hence, the probability $\alpha_{k,t,l}$ in (18) becomes:

$$\alpha_{k,t,l} = \mathcal{E}_k^{N_{e_{k,t,l}}} (1 - \mathcal{E}_k)^{L_k - N_{e_{k,t,l}}}. \quad (25)$$

2) *Noncoherent Receiver*: The channel between sensor k and the FC can no longer be modeled as a BSC. Instead, we can model it as a binary asymmetric channel, where \mathcal{E}_{1_k} is the probability that “0” bit is flipped into “1” bit, and \mathcal{E}_{2_k} is the probability that “1” bit is flipped into “0” bit. Therefore, unlike (25) for coherent receiver, the probability $\alpha_{k,t,l}$ for

noncoherent receiver should be calculated as:

$$\alpha_{k,t,l} = \prod_{i=1}^{L_k} [\mathbf{1}_{\{b_{k,l,i}=b_{k,t,i}=0\}} (1 - \mathcal{E}_{1_k}) + \mathbf{1}_{\{b_{k,l,i}=0, b_{k,t,i}=1\}} (\mathcal{E}_{1_k}) + \mathbf{1}_{\{b_{k,l,i}=1, b_{k,t,i}=0\}} (\mathcal{E}_{2_k}) + \mathbf{1}_{\{b_{k,l,i}=b_{k,t,i}=1\}} (1 - \mathcal{E}_{2_k})], \quad (26)$$

where $\mathbf{1}_{\{X\}}$ is indicator function with subscript X describing the event of inclusion. Next, we compute probabilities \mathcal{E}_{1_k} and \mathcal{E}_{2_k} in (26). Note that \mathcal{E}_{1_k} and \mathcal{E}_{2_k} do not depend on the bit index. The problem of demodulating L_k symbols (bits) sent by sensor k , based on L_k received signals, $y_{k,1}, \dots, y_{k,L_k}$ can be cast into L_k binary hypothesis testing problems, in which the channel output corresponding to each problem is:

$$y_{k,i} = \begin{cases} B_k h_k + w_{k,i}, & \mathcal{H}_{1,i} : b_{k,l,i} = 1 \\ w_{k,i}, & \mathcal{H}_{0,i} : b_{k,l,i} = 0 \end{cases}$$

for $i = 1, \dots, L_k$, where B_k is transmitted signal amplitude for sensor k . Denoting $r_{k,i}$ as the test statistics, the optimal likelihood ratio test (LRT) at the FC can be expressed as:

$$\frac{p(r_{k,i}|\mathcal{H}_{1,i})}{p(r_{k,i}|\mathcal{H}_{0,i})} \underset{\mathcal{H}_{0,i}}{\overset{\mathcal{H}_{1,i}}{\gtrless}} \frac{p(\mathcal{H}_{0,i})}{p(\mathcal{H}_{1,i})}, \quad i = 1, \dots, L_k$$

where the probabilities $p(\mathcal{H}_{1,i}) = p(b_{k,l,i} = 1)$ and $p(\mathcal{H}_{0,i}) = p(b_{k,l,i} = 0)$. Lemma 1 shows that under certain assumptions, which also hold true for our system model, $p(\mathcal{H}_{0,i}) = p(\mathcal{H}_{1,i}) = 1/2$.

Lemma 1. We have $p(\mathcal{H}_{0,i}) = p(\mathcal{H}_{1,i}) = 1/2$ under the following two assumptions: 1) the pdf of noisy observation x_k is symmetric, 2) sensor k quantizes x_k employing a uniform quantizer, and encodes the quantization level m_k according to natural binary encoding rule.

Proof. See Appendix A.

According to Lemma 1, we can state that $\mathbb{E}\{B_k^2\} = 2P_k/L_k$, where P_k is the average transmit power of sensor k . In the following, we find probabilities \mathcal{E}_{1_k} and \mathcal{E}_{2_k} for these two noncoherent receivers.

a) *Noncoherent Receiver with Known Channel Envelopes*: For this receiver, the test statistics of LRT at the FC is the envelope of channel output, i.e., $r_{k,i} = |y_{k,i}|$ and $|h_k|$ is known to the FC. Hence, given $|h_k|$, the two conditional pdfs of the test statistics under hypotheses \mathcal{H}_0 and \mathcal{H}_1 are [26]:

$$\begin{aligned} f(r_{k,i}|\mathcal{H}_0, |h_k|) &= \frac{r_{k,i}}{\sigma_{w_k}^2} e^{-\frac{r_{k,i}^2}{2\sigma_{w_k}^2}}, \\ f(r_{k,i}|\mathcal{H}_1, |h_k|) &= \frac{r_{k,i}}{\sigma_{w_k}^2} e^{-\left(\frac{r_{k,i}^2}{2\sigma_{w_k}^2} + 2\gamma_k\right)} I_0\left(\sqrt{\frac{2P_k}{L_k}} \frac{|h_k| r_{k,i}}{\sigma_{w_k}^2}\right), \end{aligned}$$

where γ_k is defined in (24) and $I_0(\cdot)$ is the zeroth-order modified Bessel function of the first kind. Since $w_{k,i}$'s are independent across L_k transmitted symbols, the random variables $r_{k,i}$ conditioned on each hypothesis and $|h_k|$ are i.i.d. for $i = 1, \dots, L_k$. Therefore, the probabilities \mathcal{E}_{1_k} and \mathcal{E}_{2_k} do not depend on bit index i . Based on equations (7-4-7) and (7-4-11) in [26], probabilities \mathcal{E}_{1_k} and \mathcal{E}_{2_k} are:

$$\mathcal{E}_{1k} = p(r_{k,i} > \zeta_k | \mathcal{H}_0, |h_k|) = e^{-\frac{\zeta_k^2}{2}}, \quad (27a)$$

$$\mathcal{E}_{2k} = p(r_{k,i} < \zeta_k | \mathcal{H}_1, |h_k|) = 1 - Q(2\sqrt{\gamma_k}, \zeta_k), \quad (27b)$$

where the decision threshold ζ_k is [26]:

$$\zeta_k = \sqrt{2 + \gamma_k},$$

and $Q(a, b)$ is the Marcum- Q function of nonnegative real numbers a and b defined by [27]:

$$Q(a, b) = \int_b^\infty x e^{-\frac{x^2+a^2}{2}} I_0(ax) dx.$$

Finally, by substituting (27) in (26), we compute $\alpha_{k,t,l}$ for noncoherent receiver with known channel envelopes.

b) Noncoherent Receiver with Known Complex Gaussian Channel Statistics: For this receiver, the test statistics of LRT at the FC is the power of channel output, i.e., $r_{k,i} = |y_{k,i}|^2$. The FC only knows that $h_k \sim \mathcal{CN}(0, 2\sigma_{h_k}^2)$. Let $\bar{\gamma}_k$ denote the average channel SNR of sensor k , where:

$$\bar{\gamma}_k = \frac{P_k \mathbb{E}\{|h_k|^2\}}{2L_k \sigma_{w_k}^2} = \frac{P_k \sigma_{h_k}^2}{L_k \sigma_{w_k}^2}, \quad (28)$$

in which we have used the knowledge of channel statistics to obtain $\mathbb{E}\{|h_k|^2\} = 2\sigma_{h_k}^2$. According to [19] we have:

$$\begin{aligned} f(r_{k,i} | \mathcal{H}_0) &= \frac{1}{2\sigma_{w_k}^2} e^{-\frac{r_{k,i}}{2\sigma_{w_k}^2}}, \\ f(r_{k,i} | \mathcal{H}_1) &= \frac{1}{2\sigma_{w_k}^2 (1 + 2\bar{\gamma}_k)} e^{-\frac{r_{k,i}}{2\sigma_{w_k}^2 (1 + 2\bar{\gamma}_k)}}, \end{aligned}$$

Again, we note that $r_{k,i}$ conditioned on each hypothesis are i.i.d. for $i=1, \dots, L_k$ and therefore the probabilities \mathcal{E}_{1k} and \mathcal{E}_{2k} do not depend on bit index i . Hence:

$$\mathcal{E}_{1k} = p(r_{k,i} > \zeta_k | \mathcal{H}_0) = \left(\frac{1}{2\bar{\gamma}_k + 1} \right)^{\frac{2\bar{\gamma}_k + 1}{2\bar{\gamma}_k}}, \quad (29a)$$

$$\mathcal{E}_{2k} = p(r_{k,i} < \zeta_k | \mathcal{H}_1) = 1 - \left(\frac{1}{2\bar{\gamma}_k + 1} \right)^{\frac{1}{2\bar{\gamma}_k}}, \quad (29b)$$

in which the decision threshold ζ_k is:

$$\zeta_k = 2\sigma_{w_k}^2 \left(1 + \frac{1}{2\bar{\gamma}_k} \right) \ln(1 + 2\bar{\gamma}_k).$$

Finally, by substituting (29) in (26), we compute $\alpha_{k,t,l}$ for noncoherent receiver with known channel statistics.

D. Finding FIM \mathbf{J} in (10)

At this point, we have all the components to write the entries $[\Lambda(\theta)]_{ij}$ in (11). Combining (17), (18) and (20)-(22), we find the following compact form representation of $[\Lambda(\theta)]_{ij}$:

$$[\Lambda(\theta)]_{ij} = \frac{1}{2\pi} \sum_{k=1}^K \frac{a_{k,i} a_{k,j}}{\sigma_{n_k}^2} G_k(\theta),$$

where the scalar $G_k(\theta)$ is:

$$G_k(\theta) = \sum_{t=1}^{M_k} \frac{\left(\sum_{l=1}^{M_k} \alpha_{k,t,l} \dot{\beta}_{k,l}(\theta) \right)^2}{\sum_{l=1}^{M_k} \alpha_{k,t,l} \beta_{k,l}(\theta)}.$$

Finally, we compute $\mathbb{E}\{\Lambda(\theta)\}$ and substitute it in (10) to

obtain matrix \mathbf{J} as:

$$\begin{aligned} \mathbf{J} &= \mathbf{C}_\theta^{-1} + \frac{1}{2\pi} \sum_{k=1}^K \frac{\mathbf{a}_k \mathbf{a}_k^T}{\sigma_{n_k}^2} \mathbb{E}\{G_k(\theta)\} \\ &= \mathbf{C}_\theta^{-1} + \frac{1}{2\pi} \mathbf{A} \text{diag} \left(\frac{\mathbb{E}\{G_1(\theta)\}}{\sigma_{n_1}^2}, \dots, \frac{\mathbb{E}\{G_K(\theta)\}}{\sigma_{n_K}^2} \right) \mathbf{A}^T. \end{aligned} \quad (30)$$

where the columns of $\mathbf{A} = [\mathbf{a}_1, \dots, \mathbf{a}_K]$ are observation gain vectors. As a benchmark, suppose all sensors' observations x_k 's are available at the FC with full precision (centralized estimation) and let \mathbf{J}_0 be the corresponding FIM. It is easy to verify that \mathbf{J}_0 admits the same decomposition as (10), that is $\mathbf{J}_0 = \mathbf{C}_\theta^{-1} + \mathbb{E}\{\Lambda_0(\theta)\}$. To find $[\Lambda_0(\theta)]_{ij}$, we start from (11) and replace $p(\hat{m}_{k,t} | \theta)$ with $f(x_k | \theta)$. Following the same procedure as we described to obtain (17) from (11), we reach:

$$[\Lambda_0(\theta)]_{ij} = \sum_{k=1}^K \int_{x_k} \left(\frac{1}{f(x_k | \theta)} \frac{\partial f(x_k | \theta)}{\partial \theta_i} \frac{\partial f(x_k | \theta)}{\partial \theta_j} \right) dx_k.$$

Since $\frac{\partial f(x_k | \theta)}{\partial \theta_i} = \frac{a_{k,i} (x_k - \mathbf{a}_k^T \theta)}{\sigma_{n_k}^2} f(x_k | \theta)$, it is straightforward to show $[\Lambda_0(\theta)]_{ij} = \sum_{k=1}^K \frac{a_{k,i} a_{k,j}}{\sigma_{n_k}^2}$. Therefore:

$$\mathbf{J}_0 = \mathbf{C}_\theta^{-1} + \mathbf{A} \text{diag} \left(\frac{1}{\sigma_{n_1}^2}, \dots, \frac{1}{\sigma_{n_K}^2} \right) \mathbf{A}^T. \quad (31)$$

V. LMMSE ESTIMATOR AND ITS MSE

Given $\hat{\mathbf{m}}$, finding the optimal MMSE estimator in closed form is mathematically intractable and requires q dimensional integrals that cannot be simplified. To curb computational complexity, we assume that the FC employs the LMMSE estimator to process $\hat{\mathbf{m}}$ and forms the estimate $\hat{\theta}$. In the following, we derive the LMMSE estimator $\hat{\theta}$ and its corresponding MSE matrix \mathbf{D} . Let vector $\check{\mathbf{m}} = \hat{\mathbf{m}} - \mathbb{E}\{\hat{\mathbf{m}}\}$. We have:

$$\begin{aligned} \hat{\theta} &= \mathbb{E}\{\theta \check{\mathbf{m}}^T\} (\mathbb{E}\{\check{\mathbf{m}} \check{\mathbf{m}}^T\})^{-1} \check{\mathbf{m}}, \\ \mathbf{D} &= \mathbf{C}_\theta - \mathbb{E}\{\theta \check{\mathbf{m}}^T\} (\mathbb{E}\{\check{\mathbf{m}} \check{\mathbf{m}}^T\})^{-1} \mathbb{E}\{\theta \check{\mathbf{m}}^T\}^T. \end{aligned} \quad (32)$$

Since θ is zero mean, we obtain $\mathbb{E}\{\theta \check{\mathbf{m}}^T\} = \mathbb{E}\{\theta (\hat{\mathbf{m}} - \mathbb{E}\{\hat{\mathbf{m}}\})^T\} = \mathbb{E}\{\theta \hat{\mathbf{m}}^T\}$. The k -th column of the cross-covariance matrix $\mathbb{E}\{\theta \hat{\mathbf{m}}^T\}$ describes the correlation between \hat{m}_k and θ . Using the Bayes' theorem we obtain:

$$\begin{aligned} \mathbb{E}\{\theta \hat{m}_k\} &= \sum_{l=1}^{M_k} \mathbb{E}\{\theta | m_{k,l}\} \mathbb{E}\{\hat{m}_k | m_{k,l}\} p(m_{k,l}), \\ \mathbb{E}\{\theta | m_{k,l}\} &= \frac{1}{p(m_{k,l})} \int_{V_\theta} \theta p(m_{k,l} | \theta) f(\theta) d\theta, \end{aligned}$$

where V_θ denotes the q -dimensional volume over which we take integral, and in the first equality we have used the fact that θ , m_k , \hat{m}_k form a Markov chain and thus, given m_k , θ and \hat{m}_k are independent. Since $p(\hat{m}_{k,t} | m_{k,l}) = \alpha_{k,t,l}$ and $p(m_{k,l} | \theta) = \beta_{k,l}(\theta)$, we reach:

$$\mathbb{E}\{\theta \hat{m}_k\} = \sum_{t=1}^{M_k} \sum_{l=1}^{M_k} \hat{m}_{k,t} \alpha_{k,t,l} \underbrace{\int_{V_\theta} \theta \beta_{k,l}(\theta) f(\theta) d\theta}_{=\mathcal{I}_{k,l}^1}, \quad (33)$$

and the expression for vector $\mathcal{I}_{k,l}^1$ is given later. By definition, the (i, j) -th entry of matrix $\mathbb{E}\{\check{\mathbf{m}} \check{\mathbf{m}}^T\}$ is:

$$[\mathbb{E}\{\tilde{\mathbf{m}}\tilde{\mathbf{m}}^T\}]_{ij} = \mathbb{E}\{\hat{m}_i\hat{m}_j\} - \mathbb{E}\{\hat{m}_i\}\mathbb{E}\{\hat{m}_j\}, \quad i, j = 1, \dots, K. \quad (34)$$

Similar to what we did in (33), to obtain $\mathbb{E}\{\hat{m}_k\}$ and diagonal entries of $\mathbb{E}\{\tilde{\mathbf{m}}\tilde{\mathbf{m}}^T\}$ (i.e., $\mathbb{E}\{\hat{m}_k^2\}$), we condition them on m_k ; however, for non-diagonal entries of $\mathbb{E}\{\tilde{\mathbf{m}}\tilde{\mathbf{m}}^T\}$ (i.e., $\mathbb{E}\{\hat{m}_i\hat{m}_j\}$), we condition them on $\boldsymbol{\theta}$. Then using (18), we get the following:

$$\mathbb{E}\{\hat{m}_i\hat{m}_j\} = \quad (35a)$$

$$\begin{cases} \sum_{t=1}^{M_k} \sum_{l=1}^{M_k} \hat{m}_{k,t}^2 \alpha_{k,t,l} \underbrace{\int_{V_\theta} \beta_{k,l}(\boldsymbol{\theta}) f(\boldsymbol{\theta}) d\boldsymbol{\theta}}_{=\mathcal{I}_{k,l}^2}, & i = j = k \\ \sum_{t_1=1}^{M_i} \sum_{t_2=1}^{M_j} \sum_{l_1=1}^{M_i} \sum_{l_2=1}^{M_j} \hat{m}_{i,t_1} \hat{m}_{j,t_2} \alpha_{i,t_1,l_1} \alpha_{j,t_2,l_2} \times \\ \underbrace{\int_{V_\theta} \beta_{i,l_1}(\boldsymbol{\theta}) \beta_{j,l_2}(\boldsymbol{\theta}) f(\boldsymbol{\theta}) d\boldsymbol{\theta}}_{=\mathcal{I}_{i,j,l_1,l_2}^3}, & i \neq j \end{cases}$$

$$\mathbb{E}\{\hat{m}_k\} = \sum_{t=1}^{M_k} \sum_{l=1}^{M_k} \hat{m}_{k,t} \alpha_{k,t,l} \mathcal{I}_{k,l}^2, \quad k = 1, \dots, K, \quad (35b)$$

where $\mathcal{I}_{k,l}^2$ and $\mathcal{I}_{i,j,l_1,l_2}^3$ are scalars. These integrals are (see Appendix B for derivations):

$$\begin{aligned} \mathcal{I}_{k,l}^1 &= \frac{\mathbf{C}_\theta \mathbf{a}_k}{\sqrt{2\pi}\sigma_k} \left(\exp\left(-\frac{u_{k,l}^2}{2\sigma_k^2}\right) - \exp\left(-\frac{u_{k,l+1}^2}{2\sigma_k^2}\right) \right), \\ \mathcal{I}_{k,l}^2 &= Q\left(\frac{u_{k,l}}{\sigma_k}\right) - Q\left(\frac{u_{k,l+1}}{\sigma_k}\right), \\ \mathcal{I}_{i,j,l_1,l_2}^3 &= Q\left(\frac{u_{i,l_1}}{\sigma_i}, \frac{u_{j,l_2}}{\sigma_j}; \rho_{ij}\right) - Q\left(\frac{u_{i,l_1}}{\sigma_i}, \frac{u_{j,l_2+1}}{\sigma_j}; \rho_{ij}\right) \\ &\quad - Q\left(\frac{u_{i,l_1+1}}{\sigma_i}, \frac{u_{j,l_2}}{\sigma_j}; \rho_{ij}\right) + Q\left(\frac{u_{i,l_1+1}}{\sigma_i}, \frac{u_{j,l_2+1}}{\sigma_j}; \rho_{ij}\right), \end{aligned}$$

in which:

$$\sigma_k = \sqrt{\sigma_{n_k}^2 + \mathbf{a}_k^T \mathbf{C}_\theta \mathbf{a}_k}, \quad \rho_{ij} = \frac{\mathbf{a}_i^T \mathbf{C}_\theta \mathbf{a}_j}{\sigma_i \sigma_j}, \quad (36)$$

and $Q(x, y; \rho)$ is a two dimensional Gaussian Q -function:

$$Q(x, y; \rho) = \frac{1}{2\pi\sqrt{1-\rho^2}} \int_x^\infty \int_y^\infty e^{-\frac{u^2+v^2-2\rho uv}{2(1-\rho^2)}} du dv.$$

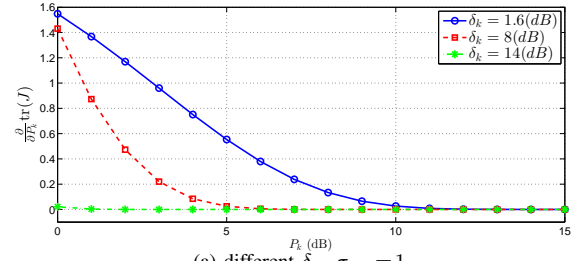
By substituting (33)-(35) in (32), the MSE matrix \mathbf{D} is computed.

As a benchmark, we consider centralized estimation case with the LMMSE estimator at the FC and let \mathbf{D}_0 denote the corresponding MSE matrix. We have:

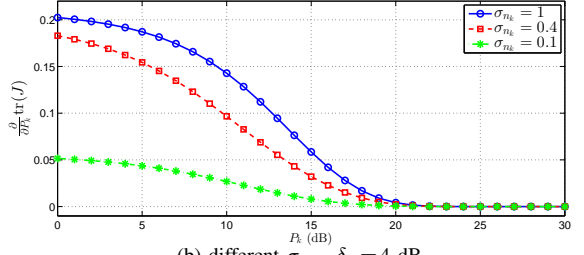
$$\mathbf{D}_0 = \mathbf{C}_\theta - \mathbb{E}\{\boldsymbol{\theta}\boldsymbol{\theta}^T\}(\mathbb{E}\{\mathbf{x}\mathbf{x}^T\})^{-1}\mathbb{E}\{\boldsymbol{\theta}\mathbf{x}^T\}^T, \quad (37)$$

where $\mathbb{E}\{\mathbf{x}\mathbf{x}^T\}$ and $\mathbb{E}\{\boldsymbol{\theta}\mathbf{x}^T\}$ respectively are, auto covariance matrix of noisy observations, and cross covariance matrix between the unknown vector and noisy observations. For linear observation model in (1) we obtain:

$$\begin{aligned} \mathbb{E}\{\boldsymbol{\theta}\mathbf{x}^T\} &= \mathbf{C}_\theta \mathbf{A}, \\ \mathbb{E}\{\mathbf{x}\mathbf{x}^T\} &= \mathbf{A}^T \mathbf{C}_\theta \mathbf{A} + \text{diag}(\sigma_{n_1}^2, \dots, \sigma_{n_K}^2), \end{aligned}$$



(a) different δ_k , $\sigma_{n_k} = 1$



(b) different σ_{n_k} , $\delta_k = 4$ dB

Fig. 2: coherent receiver: $\frac{\partial \text{tr}(\mathbf{J})}{\partial P_k}$ versus P_k (dB) for different values of (a) δ_k and (b) σ_{n_k} .

VI. POWER CONSTRAINED FISHER INFORMATION MAXIMIZATION

In this section, we address the constrained optimization problems formulated in (3) and (4). We denote the solutions obtained from solving these two power constrained Fisher information maximization problems as *FIM-max schemes*. Note that due to the cap on the total network transmit power, only a subset of the sensors might be active at each task period, which we refer to this subset as the set of active sensors $\mathcal{S}_A = \{k : P_k > 0, k = 1, \dots, K\}$.

A. Solving Optimization Problem in (3)

We adopt the Lagrange multipliers method to solve the problem and define its Lagrangian \mathcal{L} as:

$$\mathcal{L}(\lambda, \{\eta_k, P_k\}_{k=1}^K) = \text{tr}(\mathbf{J}) - \sum_{k=1}^K P_k (\lambda - \eta_k) + \lambda P_{tot}. \quad (38)$$

The Karush-Kuhn-Tucker (KKT) optimality conditions are:

$$\begin{aligned} \frac{\partial \mathcal{L}}{\partial P_k} &= \frac{\partial \text{tr}(\mathbf{J})}{\partial P_k} - \lambda + \eta_k = 0, \quad \forall k, \\ \lambda \left(\sum_{k=1}^K P_k - P_{tot} \right) &= 0, \quad \lambda \geq 0, \quad \sum_{k=1}^K P_k \leq P_{tot}, \\ \eta_k P_k &= 0, \quad \eta_k \geq 0, \quad P_k \geq 0, \quad \forall k. \end{aligned} \quad (39)$$

In the following, we argue that the objective function $\text{tr}(\mathbf{J})$ is an increasing function of P_k 's. According to (30) we find:

$$\frac{\partial \text{tr}(\mathbf{J})}{\partial P_k} = \frac{\mathbf{a}_k^T \mathbf{a}_k}{2\pi\sigma_{n_k}^2} \mathbb{E}\left\{ \frac{\partial G_k(\boldsymbol{\theta})}{\partial P_k} \right\}. \quad (40)$$

Thus, to show $\frac{\partial \text{tr}(\mathbf{J})}{\partial P_k} > 0$, we need to show $\mathbb{E}\left\{ \frac{\partial G_k(\boldsymbol{\theta})}{\partial P_k} \right\} > 0$. Our extensive simulations show that the sign of $\frac{\partial G_k(\boldsymbol{\theta})}{\partial P_k}$ for various system parameters changes and hence proving

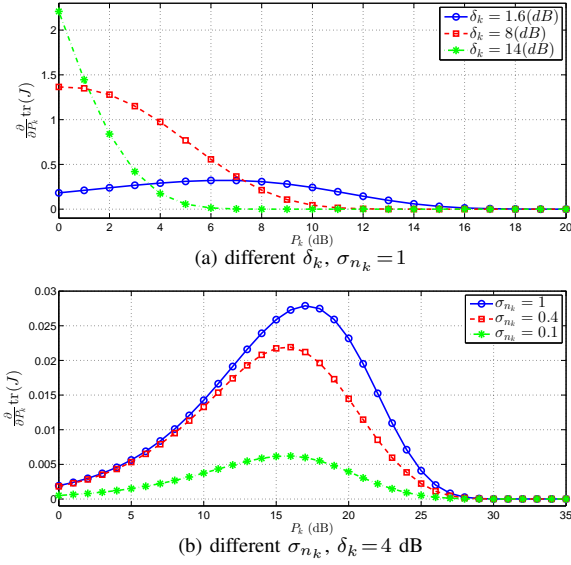


Fig. 3: Noncoherent receiver with known channel envelopes: $\frac{\partial^2 \text{tr}(\mathbf{J})}{\partial P_k^2}$ versus P_k (dB) for different values of (a) δ_k and (b) σ_{n_k} .

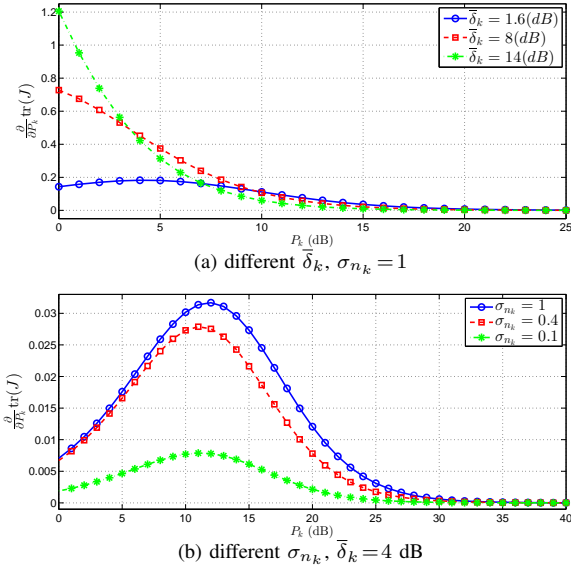


Fig. 4: Noncoherent receiver with known channel statistics: $\frac{\partial^2 \text{tr}(\mathbf{J})}{\partial P_k^2}$ versus P_k (dB) for different values of (a) δ_k and (b) σ_{n_k} .

$\mathbb{E}\{\frac{\partial G_k(\boldsymbol{\theta})}{\partial P_k}\} > 0$ analytically is infeasible. However, they indicate that $\mathbb{E}\{\frac{\partial G_k(\boldsymbol{\theta})}{\partial P_k}\} > 0$ and thus $\frac{\partial \text{tr}(\mathbf{J})}{\partial P_k} > 0$. Figs. 2–4 summarize some of our extensive simulations to demonstrate $\frac{\partial \text{tr}(\mathbf{J})}{\partial P_k} > 0$, for coherent and noncoherent receivers. For all three figures, the setup parameters are $L_k = 3$, $\mathbf{a}_k = [0.6, 0.8]^T$, $\sigma_{\theta_1} = 2$, $\sigma_{\theta_2} = 0.5$, $\rho_{\theta} = 0.5$, $\tau_k = 5.26$. Let $\delta_k = \frac{|h_k|^2}{2\sigma_{w_k}^2}$ and $\bar{\delta}_k = \frac{\sigma_{h_k}^2}{\sigma_{w_k}^2}$. For coherent receiver, Fig. 2a and Fig. 2b depict $\frac{\partial \text{tr}(\mathbf{J})}{\partial P_k}$ versus P_k for different values of δ_k and σ_{n_k} , respectively. We observe that, $\forall P_k$, and for all different values of δ_k and σ_{n_k} , we have $\frac{\partial \text{tr}(\mathbf{J})}{\partial P_k} > 0$. For noncoherent receiver with known channel envelopes, Fig. 3a and Fig. 3b depict $\frac{\partial \text{tr}(\mathbf{J})}{\partial P_k}$

versus P_k for different values of δ_k and σ_{n_k} , respectively, confirming that $\frac{\partial \text{tr}(\mathbf{J})}{\partial P_k} > 0$. For noncoherent receiver with known channel statistics, Fig. 4a and Fig. 4b depict $\frac{\partial \text{tr}(\mathbf{J})}{\partial P_k}$ versus P_k for different values of $\bar{\delta}_k$ and σ_{n_k} , respectively, confirming that $\frac{\partial \text{tr}(\mathbf{J})}{\partial P_k} > 0$.

Since $\text{tr}(\mathbf{J})$ is an increasing function of P_k 's, the Lagrange multiplier λ should be determined so that it satisfies the sum-power constraint with equality that is, $\sum_{k \in S_A} P_k = P_{\text{tot}}$. Furthermore, for the set of active sensors S_A the Lagrange multiplier $\eta_k = 0$. Hence, we can reformulate the KKT optimality conditions in (39) as:

$$\frac{\mathbf{a}_k^T \mathbf{a}_k}{2\pi\sigma_{n_k}^2} \mathbb{E}\left\{\frac{\partial G_k(\boldsymbol{\theta})}{\partial P_k}\right\} - \lambda = 0, \quad \forall k \in S_A, \quad \lambda > 0, \quad \sum_{k \in S_A} P_k = P_{\text{tot}}. \quad (41)$$

Let $\mathbf{P} = [P_1, \dots, P_K]$ be the vector of sensors' powers. The Hessian of $\text{tr}(\mathbf{J})$ with respect to \mathbf{P} is a diagonal matrix, since using (40) we find $\frac{\partial^2 \text{tr}(\mathbf{J})}{\partial P_i \partial P_j} = 0$, $i, j = 1, \dots, K$, $i \neq j$. For coherent receiver, our extensive simulations show that $\frac{\partial^2 \text{tr}(\mathbf{J})}{\partial P_k^2} < 0, \forall k$, and therefore, the Hessian is a negative semidefinite matrix. For coherent receiver Fig. 5a and Fig. 5b depict $\frac{\partial^2 \text{tr}(\mathbf{J})}{\partial P_k^2}$ versus P_k for different values of δ_k and σ_{n_k} , respectively, verifying that $\frac{\partial^2 \text{tr}(\mathbf{J})}{\partial P_k^2} < 0$. The negative semidefiniteness of the Hessian matrix means that $\text{tr}(\mathbf{J})$ is jointly concave over P_k 's. Moreover, the constraints are linear, and thus, the problem in (3) is concave. For noncoherent receivers, unlike coherent receiver, our extensive simulations show that the sign of $\frac{\partial^2 \text{tr}(\mathbf{J})}{\partial P_k^2}$ changes, and thus, $\text{tr}(\mathbf{J})$ is not always a concave function over P_k 's. Due to the integration over $\boldsymbol{\theta}$ when computing $\mathbb{E}\{\frac{\partial G_k(\boldsymbol{\theta})}{\partial P_k}\}$, the optimal solutions for λ and P_k for $k \in S_A$ cannot be obtained in a closed-form expression. Therefore, we resort to numerical Newton-Raphson algorithm to solve the set of nonlinear equations in (41). For coherent receiver, since the problem is concave, it is guaranteed that the numerical solution obtained via the algorithm is globally optimal. Therefore, only one (carefully chosen) initial point suffices to run the algorithm. However, for noncoherent receivers, since the problem is not concave, we consider multiple initial points to run the algorithm. The description of this algorithm for noncoherent receivers follows.

Let $\mathbf{z} := [\mathbf{P}, \lambda]^T$ be the vector that contains the allocated powers to sensors as well as the Lagrange multiplier λ . We let \mathbf{f} and \mathbf{g} , respectively be the gradient vector and the Jacobian matrix of the right side in (38) with respect to \mathbf{z} . We have:

$$\mathbf{f} = \left[\frac{\partial \text{tr}(\mathbf{J})}{\partial P_1} - \lambda + \eta_1, \dots, \frac{\partial \text{tr}(\mathbf{J})}{\partial P_K} - \lambda + \eta_K, P_{\text{tot}} - \sum_{k=1}^K P_k \right],$$

$$\mathbf{g} = \begin{bmatrix} \frac{\partial^2 \text{tr}(\mathbf{J})}{\partial P_1^2} & 0 & \dots & 0 & -1 \\ 0 & \frac{\partial^2 \text{tr}(\mathbf{J})}{\partial P_2^2} & \dots & 0 & -1 \\ \vdots & \vdots & \ddots & \vdots & \vdots \\ 0 & 0 & \dots & \frac{\partial^2 \text{tr}(\mathbf{J})}{\partial P_K^2} & -1 \\ -1 & -1 & \dots & -1 & 0 \end{bmatrix}. \quad (42)$$

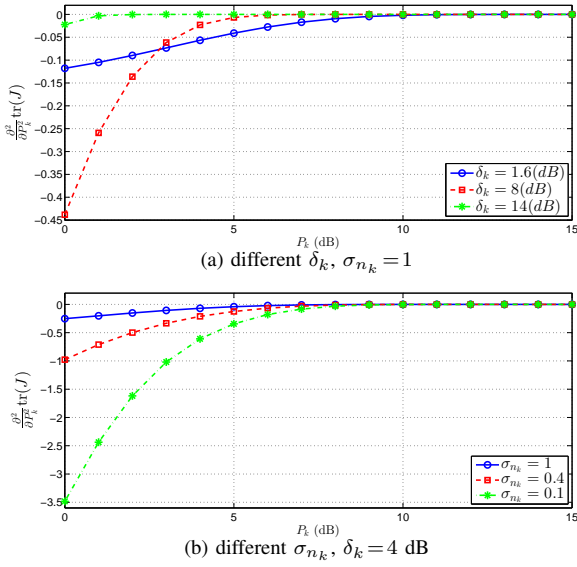


Fig. 5: coherent receiver: $\frac{\partial^2 \text{tr}(\mathbf{J})}{\partial P_k^2}$ versus P_k (dB) for different values of (a) δ_k and (b) σ_{n_k} .

Let N_i be the total number of initial points. We choose $\mathbf{z}_i^{(j)}$, $j = 1, \dots, N_i$ initial points (solutions), where j is the index of the initial points. The Newton-Raphson algorithm is carried out to obtain $\mathbf{z}_f^{(j)}$ and $T^{(j)} = \text{tr}(\mathbf{J}(\mathbf{z}_f^{(j)}))$, $j = 1, \dots, N_i$, which respectively are the final solution and the final value of the objective function obtained when the algorithm terminates, corresponding to the initial point $\mathbf{z}_i^{(j)}$. Suppose the algorithm runs for the initial point $\mathbf{z}_i^{(j)}$. Initialize with iteration index $n=0$ and $\mathbf{z}_0 = \mathbf{z}_i^{(j)}$, denote \mathbf{z}_n as the solution at n -th iteration, and $\mathbf{f}(\mathbf{z}_n)$, $\mathbf{G}(\mathbf{z}_n)$ be, respectively, the gradient vector and the Jacobian matrix evaluated at \mathbf{z}_n . At iteration n , if the Jacobian matrix $\mathbf{G}(\mathbf{z}_n)$ gets singular, or $\sum_{k \in S_A} P_k > P_{tot}$, the algorithm terminates. Otherwise, we have $\mathbf{z}_{n+1} = \mathbf{z}_n - \mathbf{G}^{-1}(\mathbf{z}_n) \mathbf{f}(\mathbf{z}_n)$. As the stopping criterion, we check whether $\frac{\|\mathbf{z}_n - \mathbf{z}_{n-1}\|}{\|\mathbf{z}_n\|} \leq \epsilon_0$, where ϵ_0 is a predetermined error tolerance, or the number of iterations exceeds a predetermined maximum I_{max} . Denote $\mathbf{z}^* = [\mathbf{P}^*, \lambda^*]^T$ as the optimal solution to this constrained optimization problem. After finding all $\{T^{(j)}\}_{j=1}^{N_i}$, \mathbf{z}^* is $\mathbf{z}_f^{(j)}$ associated with the largest value among $T^{(j)}$, $j = 1, \dots, N_i$.

B. Solving Optimization Problem in (4)

We follow the same procedure as we described above to solve (3). Specifically, we have:

$$\begin{aligned} \frac{\partial \log_2(|\mathbf{J}|)}{\partial P_k} &= \frac{1}{\ln 2} \text{tr}(\mathbf{J}^{-1} \frac{\partial \mathbf{J}}{\partial P_k}) \\ &= \frac{\mathbb{E}\{\frac{\partial G_k(\boldsymbol{\theta})}{\partial P_k}\}}{2\pi \ln 2 \sigma_{n_k}^2} \text{tr}(\mathbf{J}^{-1} \mathbf{a}_k \mathbf{a}_k^T) \end{aligned} \quad (43)$$

$$= \frac{\mathbb{E}\{\frac{\partial G_k(\boldsymbol{\theta})}{\partial P_k}\}}{2\pi \ln 2 \sigma_{n_k}^2} \mathbf{a}_k^T \mathbf{J}^{-1} \mathbf{a}_k \quad (44)$$

where we have used (30) to obtain (43) and the fact $\text{tr}(\mathbf{ABC}) = \text{tr}(\mathbf{CAB})$ to reach (44). Since $\mathbb{E}\{\frac{\partial G_k(\boldsymbol{\theta})}{\partial P_k}\} > 0$

and $\mathbf{J}^{-1} \succeq 0$ we conclude $\frac{\partial \log_2(|\mathbf{J}|)}{\partial P_k} > 0$ and thus the objective function $\log_2(|\mathbf{J}|)$ is an increasing function of P_k 's. The KKT optimality conditions are:

$$\begin{aligned} \mathbb{E}\{\frac{\partial G_k(\boldsymbol{\theta})}{\partial P_k}\} \frac{\mathbf{a}_k^T \mathbf{J}^{-1} \mathbf{a}_k}{2\pi \ln 2 \sigma_{n_k}^2} - \lambda &= 0, \quad \forall k \in S_A, \quad \lambda > 0, \\ \sum_{k \in S_A} P_k &= P_{tot}. \end{aligned} \quad (45)$$

For coherent receiver our extensive simulations show that the Hessian of $\log_2(|\mathbf{J}|)$ is a negative semidefinite matrix with respect to P_k 's, and thus, $\log_2(|\mathbf{J}|)$ is a concave function of P_k 's. However, for noncoherent receivers the sign of $\frac{\partial^2 \text{tr}(\mathbf{J})}{\partial P_k^2}$ varies for different system parameters and hence $\log_2(|\mathbf{J}|)$ is not necessarily a concave function of P_k 's. We employ Newton-Raphson algorithm with multiple initial points as we described in VI-A to solve the set of nonlinear equations in (45). A remark on the difference between power allocation based on maximization of $\text{tr}(\mathbf{J})$ and $\log_2(|\mathbf{J}|)$ follows.

Remark 1: Regarding the solution of (41) on constrained maximization of $\text{tr}(\mathbf{J})$ we note that λ^* is common and fixed for all active sensors and thus this power allocation algorithm can be implemented in a distributed fashion, i.e., the FC sends λ^* to the set of active sensors and each sensor calculates its own power P_k^* using its parameters. Unlike the solution of (41), the solution of (45) on constrained maximization of $\log_2(|\mathbf{J}|)$ cannot be implemented in a distributed fashion. In other words, the FC needs to find $\{P_k^*\}_{k \in S_A}$ and informs the active sensors of their transmit powers.

VII. NUMERICAL AND SIMULATION RESULTS

We first present some results to demonstrate the behaviors of two metrics $\text{tr}(\mathbf{J})$ and $|\mathbf{J}|$ for three types of receivers as the system setup parameters change. To illustrate the effectiveness of the proposed FIM-max schemes we plot $\text{tr}(\mathbf{J})$ and $|\mathbf{J}|$ evaluated at their corresponding optimal transmit power solutions versus P_{tot} and compare the results with those obtained from employing uniform power allocation $P_k = P_{tot}/K$. Also, we investigate the impact of network size on the power allocation and system performance.

Without loss of generality and for the simplicity of presentation, we let $K=2$ and consider a zero mean Gaussian vector $\boldsymbol{\theta} = [\theta_1, \theta_2]^T$ with $\mathbf{C}_\theta = [4, 0.5; 0.5, 0.25]$. Note that simulating a network with $K > 2$ sensors can similarly be conducted, although it takes much longer time to perform the exhaustive search needed to obtain the *globally* optimal solution of constrained optimization problem (46). Unless stated otherwise, we assume $\mathbf{a}_k = [0.6, 0.8]^T$, $\sigma_{n_k} = 1$, $\sigma_{w_k} = 1, \forall k$. We choose a proper τ_k based on the observation model and joint pdf $f(\boldsymbol{\theta})$ such that $p(|x_k| \geq \tau_k) \approx 0$. To this end, we choose $\tau_k = 3\sigma_k$ where σ_k is defined in (36). We also assume L_k 's are equal across sensors [8]. For quantization noises to be independent from each other and also from the quantizers' inputs, the step sizes Δ_k 's should be small enough (i.e., $\Delta_k \leq \sigma_k$) [25]. Since we choose $\tau_k = 3\sigma_k$, the constraint $\Delta_k \leq \sigma_k$ results in $L_k \geq \log_2 7$. We let $L_k = 3$ bits $\forall k$.

Assuming $|h_k| = 0.5$, Fig. 6 depicts $\text{tr}(\mathbf{J})$ and $|\mathbf{J}|$ versus P_{tot} for coherent receiver. The figure shows as P_{tot} increases,

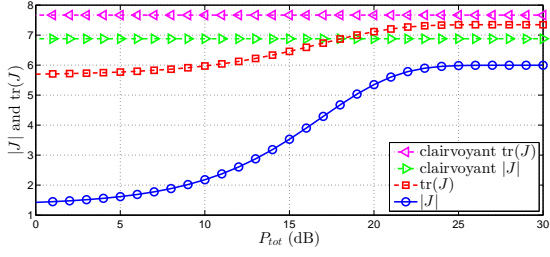
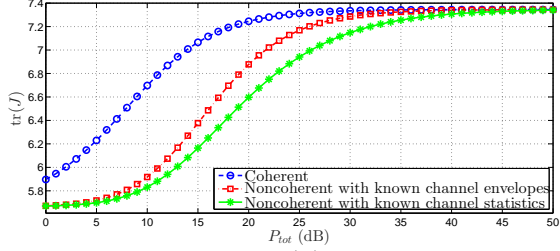
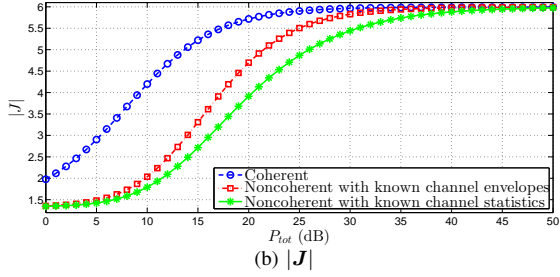


Fig. 6: $\text{tr}(\mathbf{J})$, $|\mathbf{J}|$, clairvoyant $\text{tr}(\mathbf{J})$ and clairvoyant $|\mathbf{J}|$ versus P_{tot} (dB).



(a) $\text{tr}(\mathbf{J})$



(b) $|\mathbf{J}|$

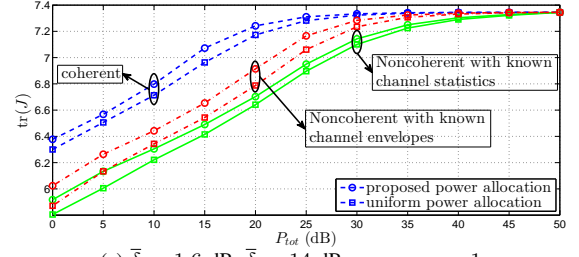
Fig. 7: (a) $\text{tr}(\mathbf{J})$ and (b) $|\mathbf{J}|$ versus P_{tot} (dB) for three types of receivers

both metrics increase and asymptotically approach their corresponding clairvoyant (i.e., centralized estimation when full precision observations are used to derive FIM and form $\hat{\theta}$). There is also a gap between each metric and its corresponding clairvoyant, which is due to quantization. The behaviors of $\text{tr}(\mathbf{J})$ and $|\mathbf{J}|$ for noncoherent receivers are the same as those of coherent receiver, hence we omitted their plots. Regarding the behaviors of the two metrics with respect to the observation model parameters, we state that $\text{tr}(\mathbf{J})$ and $|\mathbf{J}|$ increase as the variance of observation noise $\sigma_{n_k}^2$ decreases [14].

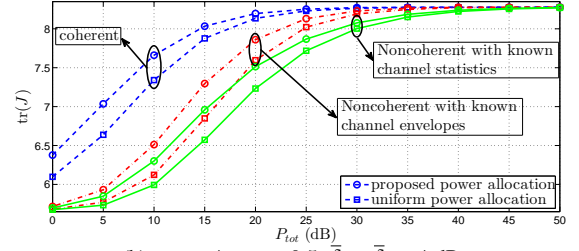
A. Homogeneous Sensor Network

We assume that all sensors have the same setup parameters and $\frac{\sigma_{h_k}}{\sigma_{w_k}} = 1$ for all k . Note that, whenever there is a comparison between the performance of different reception techniques, the results for coherent reception and noncoherent reception with known channel envelopes are obtained by taking expectation over fading channel envelope vector $|\mathbf{h}|$, such that $\mathbb{E}[|h_k|^2] = 2\sigma_{h_k}^2$ for all k .

Fig. 7a and Fig. 7b, respectively depict and compare $\text{tr}(\mathbf{J})$ and $|\mathbf{J}|$ versus P_{tot} , for three types of receivers. We observe that for a given P_{tot} , both metrics for coherent receiver are larger than those of noncoherent receivers, since the former incorporates phase information of the received signal for recovering the transmitted quantization levels. Among

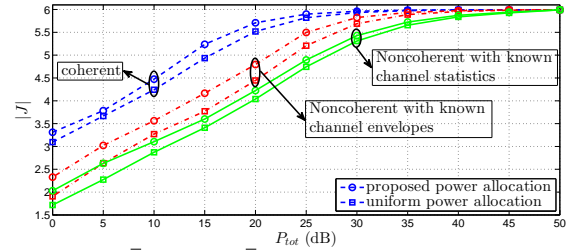


(a) $\bar{\delta}_1 = 1.6$ dB, $\bar{\delta}_2 = 14$ dB, $\sigma_{n_1} = \sigma_{n_2} = 1$

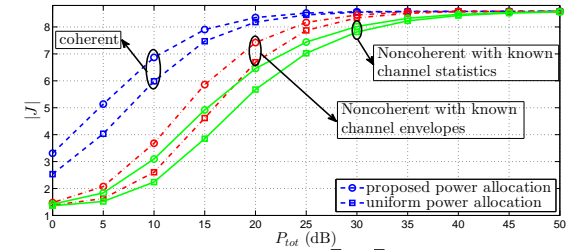


(b) $\sigma_{n_1} = 4$, $\sigma_{n_2} = 0.5$, $\bar{\delta}_1 = \bar{\delta}_2 = 4$ dB

Fig. 8: tr -bundle versus P_{tot} (dB) when (a) $\bar{\delta}_1 \neq \bar{\delta}_2$ and (b) $\sigma_{n_1} \neq \sigma_{n_2}$, for three types of receivers.



(a) $\bar{\delta}_1 = 1.6$ dB, $\bar{\delta}_2 = 14$ dB, $\sigma_{n_1} = \sigma_{n_2} = 1$



(b) $\sigma_{n_1} = 4$, $\sigma_{n_2} = 0.5$, $\bar{\delta}_1 = \bar{\delta}_2 = 4$ dB

Fig. 9: det -bundle versus P_{tot} (dB) when (a) $\bar{\delta}_1 \neq \bar{\delta}_2$ and (b) $\sigma_{n_1} \neq \sigma_{n_2}$, for three types of receivers.

the noncoherent receivers, the one with the knowledge of channel envelopes outperforms the one with known channel statistics, since the former incorporates the channel envelopes to recover the transmitted quantization levels, while the latter only exploits the channel statistics.

B. Heterogeneous Sensor Network

To investigate the effectiveness of the proposed power allocation for each type of receiver, we examine how changing the system parameters (i.e., physical layer and observation model parameters) affects the optimal power allocation and the metrics $\text{tr}(\mathbf{J})$ and $|\mathbf{J}|$ evaluated at the optimal power allocation, respectively in Figs. 8 and 9. For each type of

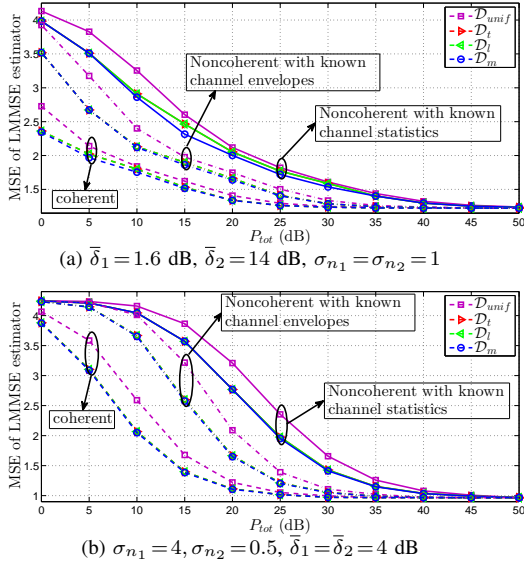


Fig. 10: MSE-bundle versus P_{tot} (dB) when (a) $\bar{\delta}_1 \neq \bar{\delta}_2$ and (b) $\sigma_{n_1} \neq \sigma_{n_2}$, for three types of receivers.

receiver and each metric, we define a bundle that contains two plots: the metric associated with the optimal transmit power obtained from solving the corresponding constrained optimization problem in section VI, and the metric associated with uniform power allocation. We call the bundles in Figs. 8 and 9 as *tr-bundle* and *det-bundle*, respectively.

Fig. 8a and Fig. 8b demonstrate *tr-bundle* versus P_{tot} . Fig. 9a and Fig. 9b demonstrate *det-bundle* versus P_{tot} . These figures demonstrate the superior performance of the proposed FIM-max scheme compared to uniform power allocation for all three types of receivers and all ranges of P_{tot} .

From a practical point of view, engineers are interested in finding the performance of the system based on MSE. Let $\mathcal{D} = \text{tr}(\mathcal{D})$, where \mathcal{D} is the MSE matrix of the LMMSE estimator given in (32). Let $\{P_k^t\}_{k \in S_A}$ and $\{P_k^l\}_{k \in S_A}$ denote, respectively, the solutions to the constrained optimization problems in (3) and (4). Suppose $\mathcal{D}_t = \text{tr}(\mathcal{D}(\{P_k^t\}_{k \in S_A}))$ and $\mathcal{D}_l = \text{tr}(\mathcal{D}(\{P_k^l\}_{k \in S_A}))$ are trace of matrix \mathcal{D} evaluated at the solutions P_k^t and P_k^l , respectively. Let $\mathcal{D}_{unif} = \text{tr}(\mathcal{D}(\{P_k = P_{tot}/K\}_{k=1}^K))$ be trace of matrix \mathcal{D} evaluated at uniform power allocation and \mathcal{D}_m be trace of \mathcal{D} evaluated at the solution of following constrained optimization problem:

$$\begin{aligned} & \underset{P_k, \forall k}{\text{minimize}} && \text{tr}(\mathcal{D}(\{P_k\}_{k=1}^K)) \\ & \text{subject to} && \sum_{k=1}^K P_k \leq P_{tot}, P_k \in \mathbb{R}^+, \forall k. \end{aligned} \quad (46)$$

We refer to the solution obtained from solving (46) as MSE-min power allocation scheme. To demonstrate the effectiveness of the proposed FIM-max schemes with respect to MSE-min as well as uniform power allocation schemes, we define *MSE-bundle* that contains four plots: \mathcal{D}_t , \mathcal{D}_l , \mathcal{D}_m and \mathcal{D}_{unif} versus P_{tot} . Note that, the closer \mathcal{D}_t or \mathcal{D}_l value is to \mathcal{D}_m , the more effective it is, in the MSE sense, to obtain power allocation from solving (3) or (4), respectively. With the

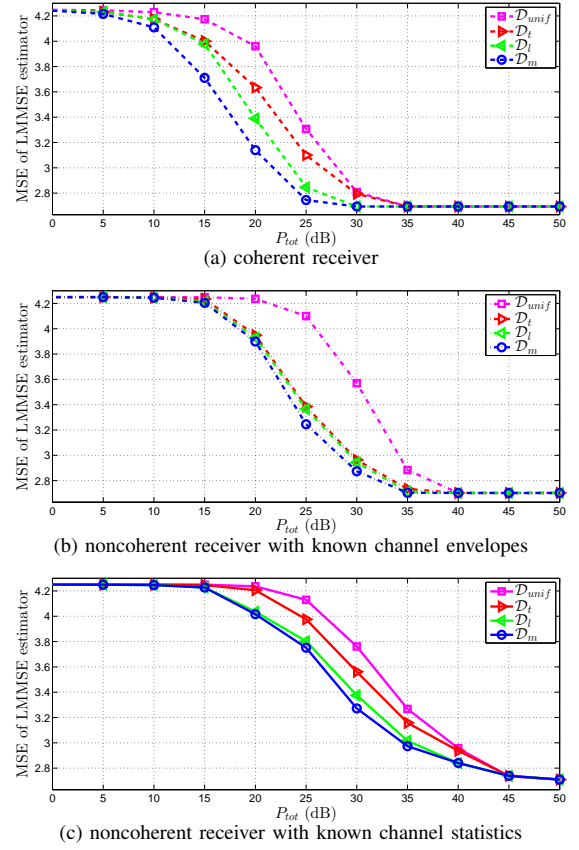


Fig. 11: MSE-bundle versus P_{tot} (dB) for (a) coherent receiver and non-coherent receiver with (b) known channel envelopes and (c) known channel statistics, $K=20$.

same setup parameters as for Fig. 8 and Fig. 9, Fig. 10a and Fig. 10b compare the *MSE-bundles* for three types of receivers, respectively, when $\bar{\delta}_1 \neq \bar{\delta}_2$, and $\sigma_{n_1} \neq \sigma_{n_2}$. In both figures, we observe $\mathcal{D}_m \leq \mathcal{D}_l = \mathcal{D}_t \leq \mathcal{D}_{unif}$ for all three receivers and all ranges of P_{tot} , which shows the very close performances of FIM-max schemes compared to MSE-min scheme. More specifically, in low-region and high-region of P_{tot} , \mathcal{D}_t and \mathcal{D}_l are much closer to \mathcal{D}_m and in moderate-region of P_{tot} , there is a small gap between them.

C. System Performance of a Randomly Deployed Network

To further evaluate the effect of network size on the system performance, we assume $K = 20$ sensors are randomly deployed in a $2m \times 2m$ field, where the origin is the center of the field, and compare the numerical results with $K = 2$ sensors. Our goal is to estimate two zero mean Gaussian external signal sources $\theta = [\theta_1, \theta_2]^T$ with $\mathcal{C}_\theta = [4, 0.5; 0.5, 0.25]$. The distance between external signal source θ_i located at (x_{t_i}, y_{t_i}) and sensor k located at (x_{s_k}, y_{s_k}) is:

$$d_{ki} = \sqrt{(x_{s_k} - x_{t_i})^2 + (y_{s_k} - y_{t_i})^2}, \quad k = 1, \dots, 20, \quad i = 1, 2$$

Let d_{0i} be the distance of θ_i from the origin. Without loss of generality, we assume $d_{01} = d_{02} = 1m$. To characterize the observation gain vectors $\mathbf{a}_k, \forall k$ in (1) we adopt an isotropic intensity attenuation model, where $\mathbf{a}_k = [(\frac{d_{01}}{d_{k1}})^n, (\frac{d_{02}}{d_{k2}})^n]^T$ and

n is the signal decay exponent which is approximately 2 for distances $\leq 1\text{km}$ [28]. We assume $\sigma_{w_k} = 1$. For coherent receiver and noncoherent receiver with known channel envelopes we let $|h_k| = 0.5, \forall k$, and for noncoherent receiver with known channel statistics we let $\sigma_{h_k} = 0.5, \forall k$.

Fig. 11 plots $MSE\text{-}bundle$ versus P_{tot} for each type of receiver separately. This figure demonstrates the superiority of FIM-max schemes, compared to uniform power allocation for all ranges of P_{tot} . Furthermore, the observation $\mathcal{D}_l \leq \mathcal{D}_t$, suggests that log-FIM-max power allocation is closer to MSE-min power allocation, compared to tr-FIM-max power allocation. This is intuitively appealing, recalling that the Bayesian FIM \mathbf{J} is not a diagonal matrix and log-FIM-max power allocation extracts and utilizes more information from \mathbf{J} , compared to tr-FIM-max power allocation.

VIII. CONCLUSIONS

We derived the Bayesian FIM matrix \mathbf{J} for distributed estimation of a Gaussian vector, when sensors transmit their digitally modulated quantized observations to the FC over power-constrained orthogonal noisy fading channels. We formulated and addressed constrained maximization of $\text{tr}(\mathbf{J})$ and $\log_2(|\mathbf{J}|)$ under the constraint on P_{tot} . We also derived the MSE of the LMMSE estimator. Through simulations we observed that both $\text{tr}(\mathbf{J})$ and $|\mathbf{J}|$ increase as P_{tot} increases. Afterwards we evaluated the system performance in terms of $\text{tr}(\mathbf{J})$, $|\mathbf{J}|$ and MSE distortion when the sensors' transmit powers are obtained from solving two aforementioned maximization problems (FIM-max schemes), and compared it with the solution obtained from minimizing the MSE of the LMMSE estimator (MSE-min scheme), and that of uniform power allocation. Numerical results demonstrated the efficiency of FIM-max schemes for different network setup parameters, as the MSE associated with FIM-max schemes are very close to that of MSE-min scheme and outperform that of uniform power allocation in all simulation scenarios. We also compared the performances of coherent and noncoherent receivers with known channel envelopes as well as known channel statistics. Numerical results revealed that coherent receiver and noncoherent receiver with known channel statistics have the best and the worst performance, respectively.

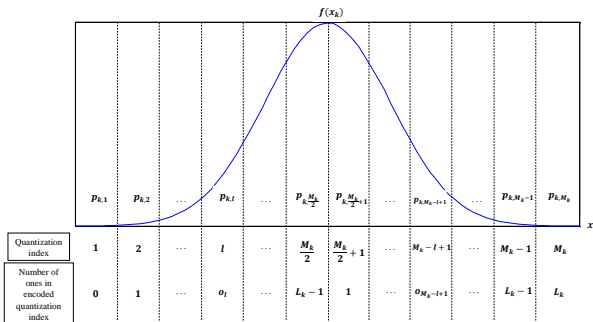


Fig. 12: Quantization and encoding of x_k with symmetric pdf.

IX. APPENDIX

A. Proof of Lemma 1

Given the assumptions made in the lemma and the number of quantization bits L_k , Fig. 12 illustrates how the noisy observation x_k is quantized and encoded. Since x_k has a symmetric pdf and quantization is uniform, defining $p(u_{k,l} < x_k \leq u_{k,l+1}) = p_{k,l}$, where $u_{k,l}$'s are quantization boundaries defined in section II, we have:

$$p_{k,l} = p_{k,M_k-l+1}, \quad l = 1, \dots, M_k$$

Moreover, for natural binary encoding of quantization indices, defining $o_{k,l}$ as the number of ones in encoded quantization index l , we can show $o_{k,l} = L_k - o_{k,M_k-l+1}$. Therefore, the prior probability $p(\mathcal{H}_{1,i})$, $i = 1, \dots, L_k$ can be computed as:

$$p(\mathcal{H}_{1,i}) = \frac{\sum_{l=1}^{M_k} o_{k,l} p_{k,l}}{L_k} = \frac{\sum_{l=1}^{M_k} [o_{k,l} p_{k,l} + (L_k - o_{k,l}) p_{k,l}]}{L_k} = \frac{1}{2}.$$

Similarly, we can show $p(\mathcal{H}_{0,i}) = 1/2$.

B. Calculation of $\mathcal{I}_{k,l}^1$ in (33), and $\mathcal{I}_{k,l}^2$ and $\mathcal{I}_{i,j,l_1,l_2}^3$ in (35)

We first calculate $\mathcal{I}_{k,l}^2$. We consider the eigenvalue decomposition of the positive definite covariance matrix $\mathbf{C}_\theta = \mathbf{U}\mathbf{\Sigma}\mathbf{U}^T$ where $|\mathbf{C}_\theta| = |\mathbf{\Sigma}|$, $|\mathbf{U}| = \pm 1$. We define $\mathbf{v} = \mathbf{U}^T \boldsymbol{\theta}$ and therefore $d\mathbf{v} = |\mathbf{U}|^q d\boldsymbol{\theta}$ [29], and also $\boldsymbol{\psi}_k = \mathbf{U}^T \mathbf{a}_k$ in which \mathbf{a}_k is observation gain vector for sensor k . Using these definitions and changes of variables along with the definition of $\beta_{k,l}(\boldsymbol{\theta})$ in (19), $\mathcal{I}_{k,l}^2$ becomes:

$$\mathcal{I}_{k,l}^2 = s_{1k} \int_{u_{k,l}}^{u_{k,l+1}} \int_{\mathbf{v} \in V_v} \exp \left\{ -\frac{1}{2} \left[\frac{(x_k - \boldsymbol{\psi}_k^T \mathbf{v})^2}{\sigma_{n_k}^2} + \mathbf{v}^T \mathbf{\Sigma}^{-1} \mathbf{v} \right] \right\} d\mathbf{v} dx_k,$$

where $s_{1k} = \frac{1}{\sqrt{(2\pi)^{q+1} |\mathbf{\Sigma}| \sigma_{n_k} |\mathbf{U}|^q}}$ and V_v denotes the q -dimensional volume over which we take integral in the new coordinate. After expanding the argument of exponential function of the integrand and using completing square, and defining:

$$\mathbf{Q}_k^{-1} = \mathbf{\Sigma}^{-1} + \boldsymbol{\psi}_k \boldsymbol{\psi}_k^T / \sigma_{n_k}^2, \quad (47a)$$

$$\boldsymbol{\omega}_k = \frac{x_k}{\sigma_{n_k}^2} \mathbf{Q}_k \boldsymbol{\psi}_k, \quad (47b)$$

$\mathcal{I}_{k,l}^2$ can be obtained as in (48), in which $s_{2k} = \frac{\sqrt{|\mathbf{Q}_k|}}{\sqrt{2\pi} |\mathbf{\Sigma}| \sigma_{n_k}}$, and for the second equality, we have used the fact that integral of pdf of Gaussian random vector \mathbf{v} over V_v is equal to 1. The term $|\mathbf{U}|^q = \pm 1$ in the denominator of s_{1k} is absorbed in the integration over \mathbf{v} , because the effects of change of variable from $\boldsymbol{\theta}$ to \mathbf{v} on V_θ to V_v and $d\boldsymbol{\theta}$ to $d\mathbf{v}$ cancel each other. Since $|\mathbf{Q}_k| = 1/|\mathbf{Q}_k^{-1}|$, using the Matrix Determinant Lemma which performs a rank-1 update to a determinant [30], we obtain:

$$|\mathbf{Q}_k| = \frac{\sigma_{n_k}^2 |\mathbf{\Sigma}|}{\sigma_{n_k}^2 + \boldsymbol{\psi}_k^T \mathbf{\Sigma} \boldsymbol{\psi}_k},$$

and therefore $s_{2k} = \frac{1}{\sqrt{2\pi (\sigma_{n_k}^2 + \boldsymbol{\psi}_k^T \mathbf{\Sigma} \boldsymbol{\psi}_k)}}$. One can also use the Binomial Inversion Lemma [30] to compute \mathbf{Q}_k as:

$$\mathbf{Q}_k = \Sigma - \frac{\Sigma \psi_k \psi_k^T \Sigma}{\sigma_{n_k}^2 + \psi_k^T \Sigma \psi_k}.$$

Substituting for \mathbf{Q}_k in (47b) and (47) in (48), it is straightforward to obtain:

$$\mathcal{I}_{k,l}^2 = s_{2k} \int_{u_{k,l}}^{u_{k,l+1}} \exp \left\{ -\frac{x_k^2}{2(\sigma_{n_k}^2 + \psi_k^T \Sigma \psi_k)} \right\} dx_k.$$

According to definition of ψ_k we have $\psi_k^T \Sigma \psi_k = \mathbf{a}_k^T \mathbf{C}_\theta \mathbf{a}_k$. Having σ_k from (36), we conclude:

$$\mathcal{I}_{k,l}^2 = Q \left(\frac{u_{k,l}}{\sigma_k} \right) - Q \left(\frac{u_{k,l+1}}{\sigma_k} \right).$$

Taking a similar approach, we can calculate $\mathcal{I}_{k,l}^1$ in (33) and $\mathcal{I}_{i,j,l_1,l_2}^3$ in (35).

ACKNOWLEDGMENT

This research is supported by NSF under grants CCF-1341966 and CCF-1319770.

REFERENCES

- [1] A. Sani and A. Vosoughi, "Resource allocation optimization for distributed vector estimation with digital transmission," in *Signals, Systems and Computers, 2014 Asilomar Conference on*, November 2014.
- [2] H. Chen and P. K. Varshney, "Performance limit for distributed estimation systems with identical one-bit quantizers," *IEEE Transactions on Signal Processing*, vol. 58, no. 1, pp. 466–471, Jan 2010.
- [3] S. Kar, H. Chen, and P. K. Varshney, "Optimal identical binary quantizer design for distributed estimation," *IEEE Transactions on Signal Processing*, vol. 60, no. 7, pp. 3896–3901, July 2012.
- [4] A. Ribeiro and G. Giannakis, "Bandwidth-constrained distributed estimation for wireless sensor networks-part i: Gaussian case," *Signal Processing, IEEE Transactions on*, vol. 54, no. 3, pp. 1131–1143, March 2006.
- [5] J.-J. Xiao, A. Ribeiro, Z.-Q. Luo, and G. Giannakis, "Distributed compression-estimation using wireless sensor networks," *Signal Processing Magazine, IEEE*, vol. 23, no. 4, pp. 27–41, July 2006.
- [6] J.-J. Xiao, S. Cui, Z.-Q. Luo, and A. Goldsmith, "Power scheduling of universal decentralized estimation in sensor networks," *Signal Processing, IEEE Transactions on*, vol. 54, no. 2, pp. 413–422, Feb 2006.
- [7] M. Chaudhary and L. Vandendorpe, "Power constrained linear estimation in wireless sensor networks with correlated data and digital modulation," *Signal Processing, IEEE Transactions on*, vol. 60, no. 2, pp. 570–584, Feb 2012.
- [8] S. Talarico, N. A. Schmid, M. Alkhawid, and M. C. Valenti, "Distributed estimation of a parametric field: Algorithms and performance analysis," *IEEE Transactions on Signal Processing*, vol. 62, no. 5, pp. 1041–1053, March 2014.
- [9] I. Nevat, G. W. Peters, and I. B. Collings, "Random field reconstruction with quantization in wireless sensor networks," *IEEE Transactions on Signal Processing*, vol. 61, no. 23, pp. 6020–6033, Dec 2013.
- [10] J. Li and G. AlRegib, "Distributed estimation in energy-constrained wireless sensor networks," *IEEE Transactions on Signal Processing*, vol. 57, no. 10, pp. 3746–3758, Oct 2009.
- [11] X. Luo and G. B. Giannakis, "Energy-constrained optimal quantization for wireless sensor networks," *EURASIP Journal on Advances in Signal Processing*, vol. 2008, no. 1, p. 462930, 2007.
- [12] A. Sani and A. Vosoughi, "Distributed vector estimation for power- and bandwidth-constrained wireless sensor networks," *IEEE Transactions on Signal Processing*, vol. 64, no. 15, pp. 3879–3894, Aug 2016.
- [13] A. Vosoughi and A. Scaglione, "On the effect of receiver estimation error upon channel mutual information," *Signal Processing, IEEE Transactions on*, vol. 54, no. 2, pp. 459–472, Feb 2006.
- [14] M. Shirazi and A. Vosoughi, "Bayesian cramer-rao bound for distributed vector estimation with linear observation model," in *2014 IEEE 25th Annual International Symposium on Personal, Indoor, and Mobile Radio Communication (PIMRC)*, 2014.
- [15] —, "Bayesian cramer-rao bound for distributed estimation of correlated data with non-linear observation model," in *2014 48th Asilomar Conference on Signals, Systems and Computers*, 2014.
- [16] S. Liu, S. P. Chepuri, M. Fardad, E. Maaazade, G. Leus, and P. K. Varshney, "Sensor selection for estimation with correlated measurement noise," *IEEE Transactions on Signal Processing*, vol. 64, no. 13, pp. 3509–3522, July 2016.
- [17] P. Venkatasubramanian, G. Mergen, L. Tong, and A. Swami, "Quantization for distributed estimation in large scale sensor networks," in *2005 3rd International Conference on Intelligent Sensing and Information Processing*, 2005.
- [18] R. Jiang and B. Chen, "Fusion of censored decisions in wireless sensor networks," *IEEE Transactions on Wireless Communications*, vol. 4, no. 6, pp. 2668–2673, Nov 2005.
- [19] O. Ozdemir, R. Niu, and P. Varshney, "Channel aware target localization with quantized data in wireless sensor networks," *Signal Processing, IEEE Transactions on*, vol. 57, no. 3, pp. 1190–1202, March 2009.
- [20] H. L. Van Trees, *Detection, Estimation, and Modulation Theory, Part I*. Wiley, 2004.
- [21] A. Vosoughi and A. Scaglione, "Everything you always wanted to know about training: guidelines derived using the affine precoding framework and the crb," *IEEE Transactions on Signal Processing*, vol. 54, no. 3, pp. 940–954, March 2006.
- [22] B. Sun, H. Chen, X. Wei, H. Wang, and X. Li, "Power allocation for range-only localisation in distributed multiple-input multiple-output radar networks - a cooperative game approach," *IET Radar, Sonar Navigation*, vol. 8, no. 7, pp. 708–718, Aug 2014.
- [23] T. M. Cover and J. A. Thomas, *Elements of Information Theory*. New Jersey: Wiley, 2006.
- [24] Z.-Q. Luo, "Universal decentralized estimation in a bandwidth constrained sensor network," *IEEE Transactions on Information Theory*, vol. 51, no. 6, pp. 2210–2219, June 2005.
- [25] B. Widrow and I. Kollar, *Quantization Noise: Roundoff Error in Digital Computation, Signal Processing, Control and Communications*. Cambridge Univ. Press, 2008.
- [26] W. R. Schwartz, M. Bennett and S. S., *Communication Systems and Techniques*. Wiley-IEEE Press, 1995, pp. 289–292.
- [27] J. I. Marcum, *Table of Q Functions*. U.S. Air Force Project RAND Res. Memo. M-339, ASTIA Document AD 1165451, RAND Corporation, Santa Monica, CA, Jan. 1, 1950.
- [28] Y. Hu and D. Li, "Energy-based collaborative source localization using acoustic micro-sensor array," *EURASIP J. Appl. Signal Process.*, vol. 2003, no. 4, pp. 321–337, March 2003.
- [29] A. Vosoughi and A. Scaglione, "Precoding and decoding paradigms for distributed vector data compression," *IEEE Transactions on Signal Processing*, vol. 55, no. 4, pp. 1445–1460, April 2007.
- [30] C. D. Meyer, *Matrix Analysis and Applied Linear Algebra*. Society for Industrial and Applied Mathematics (SIAM), 2001.

$$\mathcal{I}_{k,l}^2 = s_{1k} \int_{u_{k,l}}^{u_{k,l+1}} \int_{\mathbf{v} \in V_v} \exp \left\{ -\frac{1}{2} \left[(\mathbf{v} - \boldsymbol{\omega}_k)^T \mathbf{Q}_k^{-1} (\mathbf{v} - \boldsymbol{\omega}_k) \right] - \frac{1}{2} \left[\frac{x_k^2}{\sigma_{n_k}^2} - \boldsymbol{\omega}_k^T \mathbf{Q}_k^{-1} \boldsymbol{\omega}_k \right] \right\} d\mathbf{v} dx_k = s_{2k} \int_{u_{k,l}}^{u_{k,l+1}} \exp \left\{ -\frac{1}{2} \left[\frac{x_k^2}{\sigma_{n_k}^2} - \boldsymbol{\omega}_k^T \mathbf{Q}_k^{-1} \boldsymbol{\omega}_k \right] \right\} dx_k, \quad (48)$$